

# Acta Neuropathologica

## Convective influx/glymphatic system. Tracers injected into the CSF enter and leave the brain along separate periarterial basement membrane pathways

--Manuscript Draft--

<b>Manuscript Number:</b>	ANEU-D-17-00986R2	
<b>Full Title:</b>	Convective influx/glymphatic system. Tracers injected into the CSF enter and leave the brain along separate periarterial basement membrane pathways	
<b>Article Type:</b>	Original Paper	
<b>Keywords:</b>	intramural periarterial drainage, basement membranes, interstitial fluid, cerebrospinal fluid, glymphatic	
<b>Corresponding Author:</b>	Roxana Octavia Carare, MD, PhD University of Southampton Southampton, Hampshire UNITED KINGDOM	
<b>Corresponding Author Secondary Information:</b>		
<b>Corresponding Author's Institution:</b>	University of Southampton	
<b>Corresponding Author's Secondary Institution:</b>		
<b>First Author:</b>	Nazira Jamal Albargothy, PhD	
<b>First Author Secondary Information:</b>		
<b>Order of Authors:</b>	Nazira Jamal Albargothy, PhD	
	David A Johnston, BSc, PhD	
	Matthew MacGregor Sharp, BSc	
	Ajay Verma, MD, PhD	
	Roy Oliver Weller, MD, PhD	
	Cheryl Anne Hawkes, BSc, PhD	
	Roxana Octavia Carare, MD, PhD	
<b>Order of Authors Secondary Information:</b>		
<b>Funding Information:</b>	Biogen (FE-13227)	Prof Roxana Octavia Carare
<b>Abstract:</b>	<p>Tracers injected into CSF pass into the brain alongside arteries and out again. This has been recently termed the "glymphatic system" that proposes tracers enter the brain along periarterial "spaces" and leave the brain along the walls of veins. The object of the present study is to test the hypothesis that 1) tracers from the CSF enter the cerebral cortex along pial-glia basement membranes as there are no perivascular "spaces" around cortical arteries, 2) tracers leave the brain along smooth muscle cell basement membranes that form the Intramural Peri-Arterial Drainage (IPAD) pathways for the elimination of interstitial fluid and solutes from the brain. 2µL of 100µM soluble, fluorescent fixable amyloid β (Aβ) were injected into the CSF of the cisterna magna of 6-10 and 24-30 month-old male mice and their brains were examined 5 and 30 mins later. At 5 mins, immunocytochemistry and confocal microscopy revealed Aβ on the outer aspects of cortical arteries colocalized with α-2 laminin in the pial-glia basement membranes. At 30 mins, Aβ was colocalised with collagen IV in smooth muscle cell basement membranes in the walls of cortical arteries corresponding to the IPAD pathways. No evidence for drainage along the walls of veins was found. Measurements of the depth of penetration of tracer were taken from 11 regions of the brain. Maximum depths of penetration of tracer into the brain were achieved in the pons and caudoputamen. Conclusions drawn from the present study are that tracers injected into the CSF enter and leave the brain along separate periarterial basement membrane pathways. The exit route is along IPAD pathways in which Aβ accumulates</p>	

in cerebral amyloid angiopathy (CAA) in Alzheimer's disease. Results from this study suggest that CSF may be a suitable route for delivery of therapies for neurological diseases, including CAA.

Responses to comments from reviewers for Albargothy et al

05/05/2018

**"Convective influx/glymphatic system. Tracers injected into the CSF enter and leave the brain along separate periarterial basement membrane pathways"**

*Dear Professor Paulus,*

*Thank you for offering us the opportunity to respond to the comments from reviewers. Our responses are in italics, under each comment.*

**Reviewer #1:**

[1] Abstract line 17 delete the phrase "as there are no perivascular 'spaces' around cortical arteries" That is waving a red flag -- needlessly. Discuss that contention in the discussion, but it does not follow from the results in this paper and should not be in the abstract.

***Response***

*Thank you for this advice. However, we would prefer to retain the phrase "as there are no perivascular 'spaces' around cortical arteries" in the abstract for two reasons: 1] the abstract should be a summary of the important data that are included in the paper. Stating that there are no perivascular "spaces" around cortical arteries is part of our first hypothesis. We feel that this phrase should be included for completeness. 2] From our perspective, this phrase does not "waive a red flag" and is not contentious as we have shown and explained the absence of perivascular "spaces" around cortical arteries in a number of previous publications (see references below).*

- 1. Morris AW, Sharp MM, Albargothy NJ, Fernandes R, Hawkes CA, Verma A, Weller RO, Carare RO (2016) Vascular basement membranes as pathways for the passage of fluid into and out of the brain. Acta neuropathologica 131:725-736. doi:10.1007/s00401-016-1555-z*
- 2. Weller RO, Sharp MM, Christodoulides M, Carare RO, Møllgaard K (2018) The meninges as barriers and facilitators for the movement of fluid, cells and pathogens related to the rodent and human CNS. Acta neuropathologica 135:363-385. doi:10.1007/s00401-018-1809-z*
- 3. Zhang ET, Inman CB, Weller RO (1990) Interrelationships of the pia mater and the perivascular (Virchow-Robin) spaces in the human cerebrum. J Anat 170:111-123*

2] line 27 Wouldn't "No evidence for the tracers along the walls of veins was found." be a better summary of the results than "No evidence for drainage ....."  
The separation of hypothesis and observation is much better than in the first version.

***Response***

*Thank you for the suggestion, but we would prefer to retain the current phraseology in the abstract. Tracer is shown in a short segment of vein near the surface of the brain at 30 min in Figure 3a, so technically the phrase "No evidence for the tracers along the walls of veins was found." would be incorrect. "No evidence for drainage ....." states more accurately the findings in the present study.*

3] Separate drainage pathways of ISF and CSF. The insertion of the word "largely" on line 181 (and on line 257) helps, but the impression given is still far from that supported by the balance of all the evidence. For at least some solutes there is good evidence for drainage of ISF to CSF and for transfers of material from CSF to blood via arachnoid villi (though its relative importance is very likely to be species and age dependent). The work of people like Davson, Cserr, Bradbury and Szentisvanyi cannot be ignored simply because it is old. The references cited make an excellent case that CSF drains largely via the cribriform plate and that ISF doesn't all drain to CSF, but they do not make the case either that little or no ISF drains to CSF or that CSF drainage via the arachnoid villi is negligible. If you want to make these assertions you should either argue the case or give references to where it is done or both. Nagra 2006 *AmJPhysiol* 291, 1383 noted that in the rat a significant transfer occurs directly to blood (their early peak). On the other hand Ma et al 2017 *Nature Communications* 8, 1424 may provide some of the data you need to argue the primacy in mice of CSF drainage via perineural routes. You might also recall that Bedussi and Bakker have quite a different view (see Bedussi et al, 2017, *JCBFM* 37, 1374). You might want to reread Pollay 2010. You don't need to address questions of how ISF and CSF return to blood in this paper -- so why do so?

### **Response**

*We apologise that the relevance of separate routes for drainage of CSF and interstitial fluid (ISF) to the present paper was not made clear in lines 43 and 100. We also realise that the traditional view is that the CSF acts as a "sink" into which interstitial fluid (ISF) drains. However, the mounting evidence for largely separate drainage routes for ISF and CSF began with the work of Helen Cserr and Mike Bradbury. Helen Cserr and her colleagues emphasised the periarterial route for the drainage of radioactive tracers injected into the brain in 1984 (Szentisvanyi I, Patlak CS, Ellis RA, Cserr HF (1984) Drainage of interstitial fluid from different regions of rat brain. *American Journal of Physiology* 246:F835-844). They noted that there was only 10-15% efflux of radioactive tracer from caudate nucleus or internal capsule into the CSF, although there was more efflux from the mid brain. Szentisvanyi et al also recorded that radioactive tracer injected into the brain was only present in the walls of intracranial arteries and carotid arteries in the neck above the cervical lymph nodes and not below. Our own experiments showed that tracers injected into the brains of mice drain out of the brain along basement membranes in the walls of cerebral capillaries and arteries (Carare RO, Bernardes-Silva M, Newman TA, Page AM, Nicoll JA, Perry VH, Weller RO (2008) Solutes, but not cells, drain from the brain parenchyma along basement membranes of capillaries and arteries: significance for cerebral amyloid angiopathy and neuroimmunology. *Neuropathol Appl Neurobiol* 34:131-144. doi:10.1111/j.1365-2990.2007.00926.x). In cerebral amyloid angiopathy, the distribution of a number of amyloids in the basement membranes of cerebral capillaries and arteries exactly mirrors that of the tracers used in experimental studies. Furthermore, amyloid beta is only present in the walls of intracranial arteries and not in the carotid artery in the neck (Shinkai Y, Yoshimura M, Ito Y, Odaka A, Suzuki N, Yanagisawa K, Ihara Y (1995) Amyloid beta - proteins 1-40 and 1-42(43) in the soluble fraction of extra- and intracranial blood vessels. *Annals of neurology* 38:421-428). This suggests that the distribution of amyloid beta in relation to cerebral arteries in humans is similar to that of radioactive tracers recorded by Szentisvanyi et al. in their experiments in 1984. This chain of observations upon which the hypothesis of largely separate routes for the drainage of ISF and CSF is based is set out in detail in our previous publications and especially in Engelhardt B, Vajkoczy P, Weller RO (2017) The movers and shapers in immune privilege of the CNS. *Nature immunology* 18:123-131. doi:10.1038/ni.3666 and Engelhardt B, Carare RO, Bechmann I, Flugel A,*

Laman JD, Weller RO (2016) Vascular, glial, and lymphatic immune gateways of the central nervous system. *Acta neuropathologica* 132:317-338. doi:10.1007/s00401-016-1606-5.

Thank you for the reference to Nagra 2006 *AmJPhysiol* 291, 1383, who noted that in the rat a significant transfer of CSF occurs directly to blood (their early peak). The early peak in their paper is 10 min after injection into the CSF. Tracers injected into the CSF reach the cervical lymph nodes within 1 min (see Kida S, Pantazis A, Weller RO (1993) CSF drains directly from the subarachnoid space into nasal lymphatics in the rat. *Anatomy, histology and immunological significance. Neuropathol Appl Neurobiol* 19:480-488). Ten minutes in Nagra's study may be ample time for tracers to transfer from lymph nodes to blood.

Bedussi and Bakker did indeed have quite a different view (see Bedussi et al, 2017, *JCBFM* 37, 1374), showing that injection of relatively large volumes of tracer into the brain resulted in efflux into the CSF. The differences between the Bakker group and ours were resolved in a subsequent joint review (Bakker EN, Bacskai BJ, Arbel-Ornath M, Aldea R, Bedussi B, Morris AW, Weller RO, Carare RO (2016) Lymphatic Clearance of the Brain: Perivascular, Paravascular and Significance for Neurodegenerative Diseases. *Cell Mol Neurobiol*. doi:10.1007/s10571-015-0273-8).

Thank you for the suggestion to re-read the article by Pollay 2010. This has been done. But, as can be seen by the following paragraph and the data presented in the present response, concepts and experimental results have moved on since 2010. Quotation from Pollay 2010: "In a rat model, Weller et al also demonstrated the importance of the lymphatic drainage system in the drainage of fluid from the interstitial space of the cortex [53]. It appears that the drainage of cerebral interstitial fluid into the CSF is via the perivascular channels and subsequently entering the lymphatic system through the cribriform plate (figure 9). This supports the view that this pathway serves a primary role in the turnover of the cerebral interstitial fluid." Reference [53] is Weller RO, Kida S, Zhang ET: Pathways of fluid drainage from the brain morphological aspects and immunological significance in rat and man. *Brain Pathol* 1992, 2:277-284. This work was superseded by experiments by Roxana Carare using soluble fluorescent tracers rather than particulate Indian ink. (Carare RO, Bernardes-Silva M, Newman TA, Page AM, Nicoll JA, Perry VH, Weller RO (2008) Solutes, but not cells, drain from the brain parenchyma along basement membranes of capillaries and arteries: significance for cerebral amyloid angiopathy and neuroimmunology. *Neuropathol Appl Neurobiol* 34:131-144. doi:10.1111/j.1365-2990.2007.00926.x). This work supported more closely the findings of Helen Cserr (Szentistvanyi et al 1984) of drainage of interstitial fluid to lymph nodes.

We have re-read the section of the manuscript between lines 43 and 100 and we feel that it summarises the case put forward in our response to the reviewer's comments. We also consider that it is important to indicate the largely separate routes by which ISF and CSF drain to lymph nodes and we have added two more references that offer a more detailed explanation (Engelhardt B, Carare RO, Bechmann I, Flugel A, Laman JD, Weller RO (2016) Vascular, glial, and lymphatic immune gateways of the central nervous system. *Acta neuropathologica* 132:317-338. doi:10.1007/s00401-016-1606-5) (Engelhardt B, Vajkoczy P, Weller RO (2017) The movers and shapers in immune privilege of the CNS. *Nature immunology* 18:123-131. doi:10.1038/ni.3666)

4] pg 2 lines 201-214 These arguments completely ignore the possibility that A $\beta$  is found preferentially in the basement membranes surrounding smooth muscle cells rather than in others because it binds to components present only in those around the smooth muscle cells. Your group has evidence for binding.

## **Response**

*We agree that anything is possible. However, the presence of different chemical species of amyloid with the same distribution of basement membranes in artery walls in the different types of CAA (Revesz T, Ghiso J, Lashley T, Plant G, Rostagno A, Frangione B, Holton JL (2003) Cerebral Amyloid Angiopathies: A Pathologic, Biochemical, and Genetic View. Journal of neuropathology and experimental neurology 62:885-898) and the presence of different chemical tracers in the same basement membranes for example dextrans and ovalbumin (Carare RO, Bernardes-Silva M, Newman TA, Page AM, Nicoll JA, Perry VH, Weller RO (2008) Solutes, but not cells, drain from the brain parenchyma along basement membranes of capillaries and arteries: significance for cerebral amyloid angiopathy and neuroimmunology. Neuropathol Appl Neurobiol 34:131-144. doi:10.1111/j.1365-2990.2007.00926.x) among others (Barua NU, Bienemann AS, Hesketh S, Wyatt MJ, Castrique E, Love S, Gill SS (2012) Intrastriatal convection-enhanced delivery results in widespread perivascular distribution in a pre-clinical model. Fluids Barriers CNS 9:2. doi:10.1186/2045-8118-9-2) suggests that any binding would be for multiple substances rather than specifically for amyloid beta.*

5] pg 3 line 241 To continue playing devils advocate: Surely CAA is a process which requires foci or nucleation. If those foci are present only in the basement membranes of the smooth muscle cells, then regardless of the route of efflux, those basement membranes will be where you see the deposits.

## **Response**

*The exact mechanisms by which Abeta deposits in its fibrillar form in the lamina densa of smooth muscle cell basement membranes are not completely clear. Deposition of insoluble Abeta occurs in extracellular spaces of the brain as plaques and in capillary and artery walls. Electron microscopy has shown that, non-fibrillar and fibrillar Abeta are present in smooth muscle cell basement membranes, mainly in the lamina densa (Wisniewski HM, Wegiel J (1994) Beta-amyloid formation by myocytes of leptomenigeal vessels. Acta Neuropathol (Berl) 87:233-241) and gradually increase in amount separating the two elements of the adjacent smooth muscle cell basement membranes. (Keable A, Fenna K, Yuen HM, Johnston DA, Smyth NR, Smith C, Al-Shahi Salman R, Samarasekera N, Nicoll JA, Attems J, Kalara RN, Weller RO, Carare RO (2016) Deposition of amyloid beta in the walls of human leptomenigeal arteries in relation to perivascular drainage pathways in cerebral amyloid angiopathy. Biochimica et biophysica acta 1862:1037-1046. doi:10.1016/j.bbdis.2015.08.024).*

*The presence of fibrillary amyloid within the brain parenchyma and in vessel walls suggest that there may be multiple factors involved in the nucleation and precipitation of fibrillar Abeta. Drainage of tracers along perivascular (IPAD) pathways is impaired with age (Hawkes CA, Hartig W, Kacza J, Schliebs R, Weller RO, Nicoll JA, Carare RO (2011) Perivascular drainage of solutes is impaired in the ageing mouse brain and in the presence of cerebral amyloid angiopathy. Acta neuropathologica 121:431-443. doi:10.1007/s00401-011-0801-7) and Abeta tends to progress from soluble to fibrillar Abeta when there is stasis. A possible explanation for the deposition of fibrillary Abeta in the IPAD pathways is the age-related slowing of the perivascular clearance mechanisms from the brain-thus precipitation in both brain and the clearance pathways. Although CAA develops predominantly in the basement membranes of leptomeninges and large cortical arteries (Type 2 CAA), it is also observed in the basement membrane of capillaries (Type 1 CAA) in advanced stages of AD (Thal et al. (2008) Cerebral amyloid angiopathy and its relationship to Alzheimer's disease Acta Neuropathol. 115:599-609). Thus, the multiple sites of fibrillary Abeta the brain*

parenchyma and in the capillary and artery basement membranes suggest that it is not just basement membranes of the smooth muscle cells that are foci for nucleation of Abeta.

6] pg 3 line 260 glymphatic system not systems

**Response:** Thank you; this has been corrected

7] pg 3 line 260-162 This is an excellent example of where you need to separate results and interpretation. This should be worded "In electron microscope studies there have not been any perivascular spaces around arteries in the cerebral cortex." The cynic would continue -- of course not, you can't fix a space.

**Response**

*Although in well-fixed tissue electron microscopy does not demonstrate spaces around cortical arteries either in humans or mice, there are numerous accounts of artifactual spaces (see Weller RO, Sharp MM, Christodoulides M, Carare RO, Mollgard K (2018) The meninges as barriers and facilitators for the movement of fluid, cells and pathogens related to the rodent and human CNS. Acta neuropathologica 135:363-385. doi:10.1007/s00401-018-1809-z). Dilated perivascular spaces in the cerebral white matter and basal ganglia can be visualised by MRI (Shams S, Martola J, Charidimou A, Larvie M, Granberg T, Shams M, Kristoffersen-Wiberg M, Wahlund LO (2017) Topography and Determinants of Magnetic Resonance Imaging (MRI)-Visible Perivascular Spaces in a Large Memory Clinic Cohort. J Am Heart Assoc 6. doi:10.1161/JAHA.117.006279). Perivascular spaces in the basal ganglia can be demonstrated by electron microscopy (Pollock H, Hutchings M, Weller RO, Zhang ET (1997) Perivascular spaces in the basal ganglia of the human brain: their relationship to lacunes. J Anat 191 ( Pt 3):337-346), as can perivascular spaces in the white matter (Carare in press).*

*The following has been inserted into the manuscript on **Page 3 Lines 105-108** ".....although dilated perivascular spaces do develop in other parts of the brain such as cerebral white matter and the basal ganglia (Shams S, Martola J, Charidimou A, Larvie M, Granberg T, Shams M, Kristoffersen-Wiberg M, Wahlund LO (2017) Topography and Determinants of Magnetic Resonance Imaging (MRI)-Visible Perivascular Spaces in a Large Memory Clinic Cohort. J Am Heart Assoc 6. doi:10.1161/JAHA.117.006279). Perivascular spaces in the basal ganglia can be demonstrated by electron microscopy (Pollock H, Hutchings M, Weller RO, Zhang ET (1997) Perivascular spaces in the basal ganglia of the human brain: their relationship to lacunes. J Anat 191 ( Pt 3):337-346)"*

8] The nanoparticles are found in the basement membranes, they are not (or at least have not been) seen to pass along them. You can of course, assert the interpretation that "the observation of probes penetrating via perivascular spaces" was in fact "the observation of probes that had penetrated via basement membranes" -- but you don't have evidence for one or the other. You cannot infer in vivo from fixed tissue without careful argument and that is still missing. (Please remember that when Davson took on the electron microscopists on extracellular spaces, Davson won!)

**Response**

*The problem here is that we have been unable to demonstrate the perivascular "spaces" around cortical arteries in well-fixed tissue in electron microscope preparations whereas we have been able to demonstrate perivascular spaces around arteries in the basal ganglia. We*

agree that flow of nanoparticles into the brain along pial-glial basement membranes has not been directly visualised. However, the most logical explanation for the presence of nanoparticles in pial glial basement membranes following injection of the nanoparticles into the CSF is that they entered by this route. *Page 3, line 116* has been modified by the insertion of the words "most probable".

9] pg 3 lines 271-277. I support the second referee's opinion on the status of these objectives. You have not achieved these objectives. For the first, entry could still be via free spaces. For the second see the comments below. What you have done is well worth doing, but it has not (yet) answered these questions. What you have done is show the locations of the tracers at two time points. There are arguments you can give which support the existence of two separate pathways (itself an important result) but they don't yet prove it as you don't yet have evidence of outward flow along the inner pathway. At the late time point there would only be a little tracer in the outward pathway regardless of whether or not it is the major route of efflux. If it is, it will be flushed into CSF quickly and hence will have only a low concentration.

### **Response**

*Thank you for your interesting interpretation of our results. We have presented our current observations i.e. at 5 min after injection of tracer into the CSF it is present in the pial glial basement membrane on the outer aspect of artery walls. The tracer co-localises with proteins within the pial glial basement membrane. At 30 min after injection, tracer is present in the basement membranes of capillaries in the old mice and in smooth muscle cells in the tunica media of arteries in old and young mice in a similar distribution to the IPAD pathway identified by intracerebral injection studies and by CAA. We have put forward what we feel is a reasonable interpretation of these findings and a working hypothesis that tracer enters the brain from the CSF along pial-glial basement membranes and leaves the brain along IPAD pathways.*

[10] lines 278-281 The third objective is much more objective -- and it has been achieved.

[11] lines 280-281 You do yourselves down. This is an important study of the basic physiology of the process. Don't justify it with just an application. Perhaps "An important practical application of this study relates to drug delivery from the CSF which will be ....."

### **Response**

*Our results are mostly relevant to intrathecal drug delivery, so we have expanded the discussion to reflect this. Page 11 lines 445-454*

[12] pg 11 lines 863 to 870 There is a more conventional explanation for the decrease in A $\beta$  reaching CSF once plaques have formed. The soluble A $\beta$  concentrations in the parenchyma are thought (see Cirrito, J. R. et al (2003) J. Neurosci. 23: 8844-8853) to be lower once plaques are formed, because the plaques take up a significant fraction of the A $\beta$  that is being produced. Before plaques form ISF is super-saturated in the "soluble" forms of A $\beta$  -- the plaques need to be seeded.

## **Response**

*Thank you for pointing out the paper by Cirrito, J. R. et al (2003) from Holtzman's group. There are other papers recording that in transgenic APP mice soluble A beta levels in the brain are continually elevated, increasing 4-fold at 2 months and 33-fold in the APP23 Tg mice at 20 months of age when compared to the control mice (Kuo YM, Beach TG, Sue LI, Scott S, Layne KJ, Kokjohn TA, Kalback WM, Luehrs DC, Vishnivetskaya TA, Abramowski D, Sturchler-Pierrat C, Staufienbiel M, Weller RO, Roher AE (2001) The evolution of A beta peptide burden in the APP23 transgenic mice: implications for A beta deposition in Alzheimer disease. Mol Med 7:609-618). In mice there is overexpression of APP, but elevation of soluble Abeta levels has been recorded at post-mortem in brains from demented patients with Alzheimer's disease (McLean CA, Cherny RA, Fraser FW, Fuller SJ, Smith MJ, Beyreuther K, Bush AI, Masters CL (1999) Soluble pool of Abeta amyloid as a determinant of severity of neurodegeneration in Alzheimer's disease. Annals of neurology 46:860-86; Lue LF, Kuo YM, Roher AE, Brachova L, Shen Y, Sue L, Beach T, Kurth JH, Rydel RE, Rogers J (1999) Soluble amyloid beta peptide concentration as a predictor of synaptic change in Alzheimer's disease. The American journal of pathology 155:853-862).*

*It is possible that age-related impairment of IPAD results in loss of homeostasis in the brain parenchyma and that the rise in the level of soluble Abeta in Alzheimer's disease reflects such loss of homeostasis (Weller RO, Hawkes CA, Carare RO, Hardy J (2015) Does the difference between PART and Alzheimer's disease lie in the age-related changes in cerebral arteries that trigger the accumulation of Abeta and propagation of tau? Acta neuropathologica 129:763-766. doi:10.1007/s00401-015-1416-1)*

[13] These results can be interpreted in a number of ways, one of which you have chosen to present as the inevitable conclusion of your observations. If, as you say, the tracer is entering the tissue along the external basement membrane at the time of the 5 min snapshot and leaving the tissue along the smooth muscle cells at the time of the 30 min snapshot, then there should have been an intermediate time and place for the tracer to have been in transit from one to the other. Where and when? If the transit from one to the other occurs along the length of the arteries/arterioles there is one interpretation, if it occurs only at the capillaries one has the interpretation you've given. Your present discussion is leaping ahead of the results until you know which. Careful measurements of relative concentrations along the two pathways as a function of time should be able to resolve this issue. It sounds like a lot of work!

## **Response**

*We agree that, ideally, measurements should be taken at every conceivable time point and at every conceivable point in the anatomy of the inflow and outflow system for tracers in the CSF entering and leaving the brain. At the moment we have snapshots at 5 min and 30 min after injection of tracer into the CSF and it is from these snapshots that we have formulated our working hypothesis.*

*Drainage of tracers out of the brain following intracerebral injection is impaired with age (Hawkes CA, Hartig W, Kacza J, Schliebs R, Weller RO, Nicoll JA, Carare RO (2011) Perivascular drainage of solutes is impaired in the ageing mouse brain and in the presence of cerebral amyloid angiopathy. Acta neuropathologica 121:431-443. doi:10.1007/s00401-011-0801-7 , such that a greater number of capillaries show tracer in their basement membranes at a set time following intracerebral injection. In the present study, tracer is present in the basement membranes of capillaries at 30 min following injection of tracer into the CSF in the older age group of mice. This gives some indication of the possible pathway*

*for drainage of tracers out of the brain. We have used this information to support our working hypothesis that the tracers are draining along basement membranes of capillaries and arteries as they pass out of the brain along the IPAD pathway. Furthermore, the presence of tracer in astrocyte processes within the brain parenchyma (as reported in the present paper) suggests that tracer has entered the interstitial fluid and been taken up by these cells.*

**Reviewer #2:**

In their revision, the authors have substantially revised the presentation of their findings, but have conducted no additional experiments to address the comments of either Reviewer 1 or Reviewer 2. Thus, while the self-confirmatory tone of the prior submission is largely muted, the most important criticisms of these two reviewers from the prior submission remain largely unresolved.

1] Both reviewers noted that that the technical approaches and the two time points utilized in this study prevent any sense of the direction of tracer movement from being defined. Given that this is one of the central controversies in the field, addressing this issue of key importance. In response, the authors have now cited a prior study from their group which suffers from the same technical limitations, and a 2-photon microscopy study using a very different injection paradigm than either their own or those from Nedergaard and colleagues. This latter study uses a pressure injection approach (5-20 PSI for 10-30 s) to introduce tracer for intravital imaging. While this approach may be relevant to the field of convection-enhanced delivery, it is unclear if the results are relevant to the physiology movement of fluid and solutes out of brain tissues, which the authors of the present study implicitly note by using a 'small' volume of 0.5ul. In their response to Reviewer 2, the authors note the technical difficulties in conducting these studies. But that is the very reason that this question is important to answer. A study that moved the field forward would devise a clever way to do this.

2] Related to this issue, is the inability to distinguish the route of tracer movement between the 5 and 30 min time points, including resolving between organized 'flow' and simple distribution by diffusion. This is a second key element of controversy in the field that the authors do not address.

***Responses to points [1-2]***

*We thank the reviewer #2 for the insightful comments and we will certainly bear them in mind for the design of future experiments.*

*The objectives of the experiments reported in the present paper were 1] to demonstrate in young and aged mice that the pial-gliial basement membranes are the entry route into the brain for soluble tracers from the CSF and 2] to test the hypothesis that tracers entering the brain from the CSF drain out of the brain parenchyma along the IPAD pathways. 3] to determine the range of depths of penetration of tracer alongside arteries in different regions of the brain and for the time points of 5 and 30 min in young and aged mice. We consider that we have achieved these objectives.*

*Furthermore we have tried to answer to points raised in by reviewers #1 and #2 in their first reviews. We are sorry if we had not been able to answer all the criticisms but we have*

*answered questions to the best of our ability. Some of the questions raised in the second reviews by reviewer #2 have been answered in our responses to reviewer #1.*

3] In response to Reviewer 1's critiques (#13) concerning the possibility of artifactual vascular labeling resulting from pressure injection ascribed to Iliff et al. (2012) being a possible confound to their own data, the authors simply cite yet more defects from the Iliff study. It is the veracity of the present study's findings that are the subject of the review. Pointing to the defects in another study doesn't nullify the impact those defects for the study in question.

### **Response**

*With regard to our mention of Iliff's study, we are putting forward possible reasons for the discrepancies between Iliff's findings and our findings in the present paper. We feel that this is a valid insertion.*

[4] In response to this reviewer's questions regarding the strikingly low variance observed in these studies, the authors have changed the presentation so that the data are not shown with log-transformation. This doesn't address the general surprise at observing such large effects with such small (n=3) sample sizes. A post-hoc power analysis of this data does not ameliorate these concerns, given that if the data were flawed in some way systematic way, so too would be the power analysis.

### **Response**

*As described in the manuscript, "the distance of the A $\beta$ -positive blood arteries from the surface or base of the brain was measured by drawing two perpendicular lines (one travelling in the direction of the vessel and a tangent of the surface/base of the brain; see supplementary Figure 1) and determining the distance of the vessel from the point at which the two lines meet." These measurements were applied consistently across all brain regions that were analysed in young and aged animals. Because the quantification data in some brain areas were not normally distributed, log transformation was applied to all groups and analysed using one- or two-way ANOVA with Sidak's posthoc test to control for multiple comparisons. These log transformed data were presented in the original manuscript not to obscure variations between groups but to accurately reflect the data as analysed. Based on the recommendation from Reviewer 1, the raw values (mean  $\pm$  S.E.M from individual animals) were presented in the figures of the revised manuscript. As previously indicated, post-hoc power calculations indicate that the n=3 used in the study was sufficient to detect a significant difference between brain regions and age groups (86-97% power,  $\alpha = 0.05$ ) due to large effect sizes (Cohen's  $f = 4.06-5.76$ ) that are underpinned by biological variations in regional and age-related clearance of solutes, as previously reported (Szentistvanyi I, Patlak CS, Ellis RA, Cserr HF (1984) Drainage of interstitial fluid from different regions of rat brain. *American Journal of Physiology* 246:F835-844; Hawkes CA, Hartig W, Kacza J, Schliebs R, Weller RO, Nicoll JA, Carare RO (2011) Perivascular drainage of solutes is impaired in the ageing mouse brain and in the presence of cerebral amyloid angiopathy. *Acta neuropathologica* 121:431-443). The method of quantification, statistical analyses and*

*presentation of the data in the Figures are all described in full in the revised manuscript (Page 5-6 Lines 202-226).*

[5] In response to reviewer comments concerning both the effect of anesthesia, and of mode of injection, particularly when seeking to make a comparison with other parallel studies, the authors essentially reply that that they will 'take note' of these differences and will 'bear [them] in mind' in future experiments. However, these are issues that confound the present findings and their interpretation, and as such, they should be addressed in the present study.

### **Response**

*We recognise that we have not measured changes in CSF pressure in the cisterna magna during injections or estimated the changes in pressure over the superior surfaces of the cerebral hemispheres at a distance from the cisterna magna. Nevertheless, we consider that our observations are valid and that our findings support our working hypothesis that tracer enters the brain from the CSF along pial-glia basement membranes and leaves the brain along the IPAD pathway.*

*With regard to anaesthesia - we have undertaken experiments testing the effects on heart rate, pulse, distension, breath rate, breath distension and arterial oxygen saturation for isoflurane and for another common anaesthetic used in rodent studies: 10mg/ml ketamine with 1mg/ml xylazine. The result is displayed in online resource 1 and demonstrates that isoflurane does not reduce the heart rate or oxygen saturation as does ketamine. As all groups were anaesthetised with isoflurane, we conclude that the effects observed are not due to an effect of anaesthesia. (see page 4 lines 148-151; page 14 lines 569-575)*

[Click here to view linked References](#)

1 Convective influx/glymphatic system. Tracers injected into the CSF enter and leave  
2 the brain along separate periarterial basement membrane pathways

3 Nazira J Albargothy<sup>1</sup>, David A Johnston<sup>1</sup>, Matthew MacGregor-Sharp<sup>1</sup>, Roy O  
4 Weller<sup>1</sup>, Ajay Verma<sup>2</sup>, Cheryl A Hawkes<sup>3\*</sup>, Roxana O Carare<sup>1\*</sup>

5 <sup>1</sup>Faculty of Medicine, University of Southampton, U.K

6 <sup>2</sup>Biogen, U.S.A

7 <sup>3</sup>Open University, U.K

8 \*Contributed equally to the study

9 Corresponding Author and email address

10 Key words: intramural periarterial drainage, basement membranes, interstitial fluid,  
11 cerebrospinal fluid, glymphatic

## 12 **Abstract**

13 Tracers injected into CSF pass into the brain alongside arteries and out again. This  
14 has been recently termed the “glymphatic system” that proposes tracers enter the  
15 brain along periarterial “spaces” and leave the brain along the walls of veins. The  
16 object of the present study is to test the hypothesis that 1) tracers from the CSF enter  
17 the cerebral cortex along pial-glia basement membranes as there are no  
18 perivascular “spaces” around cortical arteries, 2) tracers leave the brain along  
19 smooth muscle cell basement membranes that form the Intramural Peri-Arterial  
20 Drainage (IPAD) pathways for the elimination of interstitial fluid and solutes from the  
21 brain. 2µL of 100µM soluble, fluorescent fixable amyloid β (Aβ) were injected into the  
22 CSF of the cisterna magna of 6-10 and 24-30 month-old male mice and their brains  
23 were examined 5 and 30 mins later. At 5 mins, immunocytochemistry and confocal  
24 microscopy revealed Aβ on the outer aspects of cortical arteries colocalized with α-2  
25 laminin in the pial-glia basement membranes. At 30 mins, Aβ was colocalised with  
26 collagen IV in smooth muscle cell basement membranes in the walls of cortical  
27 arteries corresponding to the IPAD pathways. No evidence for drainage along the  
28 walls of veins was found. Measurements of the depth of penetration of tracer were  
29 taken from 11 regions of the brain. Maximum depths of penetration of tracer into the  
30 brain were achieved in the pons and caudoputamen. Conclusions drawn from the  
31 present study are that tracers injected into the CSF enter and leave the brain along  
32 separate periarterial basement membrane pathways. The exit route is along IPAD  
33 pathways in which Aβ accumulates in cerebral amyloid angiopathy (CAA) in  
34 Alzheimer’s disease. Results from this study suggest that CSF may be a suitable  
35 route for delivery of therapies for neurological diseases, including CAA.

36

37

38

39 **Introduction:**

40 Apart from blood, there are two major extracellular fluids associated with the brain  
41 and spinal cord, namely CSF in the ventricles and subarachnoid spaces, and  
42 interstitial fluid (ISF) in the extracellular spaces of the brain and spinal cord. CSF and  
43 ISF appear to drain from the brain along largely separate pathways to regional lymph  
44 nodes [11]. Tracers injected into the CSF drain from the subarachnoid space to  
45 cervical lymph nodes by channels that pass through the cribriform plate and join  
46 lymphatic channels in the nasal submucosa [18, 20, 27]. Similarly, there is lymphatic  
47 drainage of CSF alongside cranial and spinal nerves and into lymphatics in the dura  
48 mater [3, 8, 11, 22].

49 There are no conventional lymphatic vessels in the brain parenchyma, but there is  
50 lymphatic drainage of ISF to cervical lymph nodes [11, 39]. When minute amounts of  
51 radioactive tracer are injected into deep grey matter of the rat brain, they drain to  
52 cervical lymph nodes along the walls of cerebral and intracranial arteries [39]. High-  
53 resolution studies using formalin-fixable fluorescent tracers suggest that the drainage  
54 pathways for ISF and solutes from the brain are the basement membranes in the  
55 walls of cerebral capillaries and arteries [4]. Injection of fluorescent tracer in small  
56 amounts of 0.5  $\mu$ L through fine 50  $\mu$ m glass cannulae ensures that no tracer leaks  
57 into the CSF [4]. At 5 min following these injections, tracers are within the basement  
58 membranes of cerebral capillaries and in basement membranes around smooth  
59 muscle cells in the tunica media of cerebral arteries. By 30 mins post-injection, no  
60 tracer remains in basement membranes in the walls of capillaries or arteries but the  
61 course of each artery involved is outlined by perivascular macrophages containing  
62 tracer [4].

63 Flow of tracer along smooth muscle cell basement membranes in the walls of  
64 arteries has been demonstrated by *in vivo* multiphoton imaging [2]. Ultrastructural  
65 studies have shown that, following injection of soluble amyloid- $\beta$  (A $\beta$ ) into the mouse  
66 brain as a tracer, A $\beta$  pervades the extracellular spaces of the brain and is in  
67 continuity with A $\beta$  within capillary basement membranes [24]. In artery walls,  
68 however, tracer injected into the brain parenchyma is confined to basement  
69 membranes surrounding smooth muscle cells in the tunica media and is not observed  
70 in basement membranes associated with either endothelial cells or with pial-glial  
71 basement membranes on the external aspects of the tunica media [4]. It appears,  
72 therefore, that tracer is unlikely to enter artery walls either via the endothelium or  
73 radially from the brain parenchyma through the glia limitans. From these  
74 observations it appears that tracers in the ISF pass from the brain parenchyma into  
75 basement membranes of capillaries and flow out of the brain along smooth muscle  
76 cell basement membranes in the walls of arteries [2, 4]. This pathway has been  
77 termed the Intramural Peri-Arterial Drainage (IPAD) pathway. The relevance of IPAD  
78 to neurodegenerative disease in humans is emphasised by the pattern of deposition  
79 of A $\beta$  in the walls of cerebral capillaries and arteries as cerebral amyloid angiopathy  
80 (CAA). In the early stages of CAA, the pattern of deposition of A $\beta$  corresponds,  
81 exactly, with the IPAD pathways identified by fluorescent tracer studies in the mouse  
82 [14, 19, 29].

83 Although tracers and A $\beta$  in CAA outline the endothelial/glial basement membranes

84 around capillaries, tracers and A $\beta$  are limited to basement membranes around  
85 smooth muscle cells in the tunica media of arteries within the brain and  
86 leptomeninges. Neither the endothelial basement membranes nor the outer pial-glia  
87 basement membranes are outlined by tracer or by the deposition of A $\beta$  [4].

88 There is, therefore, evidence from experimental studies and from CAA that IPAD is a  
89 physiological pathway for drainage of ISF and solutes from the brain. Evidence from  
90 radioactive tracer studies [36] and from the drainage of A $\beta$  from the brain [26]  
91 strongly support the concept that the IPAD route is the lymphatic drainage pathway  
92 for ISF and solutes from rodent and human brain. Radioactive tracers injected into the  
93 brain are present in the walls of intracranial arteries but not in the carotid artery in the  
94 neck [36]. Furthermore, biochemical analyses of A $\beta$  in the walls of human arteries  
95 from 20 years of age onwards detected increasing amounts of A $\beta$  in the walls of  
96 intracranial arteries with age but very little A $\beta$  was detected at any age in the  
97 extracranial carotid arteries in the neck [33]. These results would correlate with A $\beta$   
98 draining from the brain along artery walls and passing to lymph nodes closely applied  
99 to the carotid artery below the base of the skull [7].

100 Despite the largely separate drainage pathways for CSF and ISF, the two fluids do  
101 mix within the brain. Tracers injected into the CSF pass into the brain and spinal cord  
102 tissue along the outer aspects of arteries and this system has been variously named  
103 as convective tracer influx and the glymphatic system [17, 30]. Electron microscope  
104 studies have shown that there are no perivascular spaces around arteries in the  
105 cerebral cortex [23, 37, 40] although dilated perivascular spaces do develop in other  
106 parts of the brain such as cerebral white matter and the basal ganglia [32].  
107 Perivascular spaces in the basal ganglia have been demonstrated by electron  
108 microscopy [28].  
109

110 When nanoparticles are injected as tracers into the CSF of mice, they appear to pass  
111 into the brain along the basement membrane between the coatings of pia mater on  
112 the outer aspect of cortical arteries and the glia limitans on the surface of the brain,  
113 the pial-glia basement membrane [24]. Previous studies have suggested that tracers  
114 injected into the CSF pass into the brain along assumed periarterial “spaces” and  
115 drain out of the brain along the walls of veins [17]. Having defined by electron  
116 microscopy the most probable entry pathway for particulate tracers passing into the  
117 brain from the CSF as the pial-glia basement membrane, we used injections of  
118 tracer into the CSF of the cisterna magna of mice to achieve three objectives. Our  
119 first two major objectives in the present study are: (1) to demonstrate by  
120 immunocytochemistry that the pial-glia basement membranes are the entry route  
121 into the brain for soluble tracers from the CSF and (2) to test the hypothesis that  
122 tracers entering the brain from the CSF drain out of the brain parenchyma along the  
123 IPAD pathways. Groups of mice were examined 5 min and 30 min after injection of  
124 fluorescent A $\beta$  tracer into the cisterna magna of young 2-10 week and aged 24-30  
125 month old mice.

126 The third major objective in this study is to determine the range of depths of  
127 penetration of tracer alongside arteries in different regions of the brain and for the  
128 time points of 5 and 30 min in young and aged mice. The importance of this study  
129 relates to drug delivery from the CSF and will be dealt with further in the discussion.

130

131 **Materials and Methods:**

132 **Animals**

133 Male C57BL/6 mice 6–10 weeks (young) and 24–30 months (old) were housed at the  
134 Biomedical Research Facility (BRF) at Southampton General Hospital (Southampton,  
135 UK). All mice were housed in groups of 4–10. They were kept under standard 12-hr  
136 light/dark cycle and fed a standard RM1 chow diet (SDS, UK) and water ad libitum.  
137 Environmental enrichment consisted of wooden sticks, red plastic tunnels and other  
138 bedding. All procedures were carried out in accordance with animal care guidelines  
139 stipulated by the United Kingdom Animals (Scientific Procedures) Act 1986, Home  
140 Office licence (PPL 30/3095).

141 **Anaesthesia**

142 C57BL/6 mice were anaesthetised using a standard isoflurane anaesthesia system.  
143 An anaesthesia induction chamber was precharged with 5% isoflurane for 5 minutes  
144 and the oxygen flow meter was set to approximately 1.7 lmin<sup>-1</sup> with the indicator ball  
145 floating between the 1 and 2 hash marks. The isoflurane vaporizer was then reduced  
146 to 1–2 % and the mouse was left in the chamber for 3–5 minutes. **We chose**  
147 **isoflurane after our pilot experiments in n=3 wild type mice determined that isoflurane**  
148 **did not reduce the heart rate or oxygen saturation in C57BL/6 mice to the same**  
149 **degree as our previous anaesthetic (ketamine and xylazine), see Online Resource 1.**  
150 The level of anaesthesia was monitored using the pedal withdrawal reflex response.  
151 Once the mouse reached a surgical plane of anaesthesia (no reflex) it was  
152 transferred from the induction chamber onto a surgical bed with a breathing device  
153 and mask that supplied a constant flow of 1 to 2 % isoflurane and 1.7 lmin<sup>-1</sup> oxygen  
154 to keep the animal safely anaesthetised during the surgical procedure. The core body  
155 temperature was monitored using a rectal probe and maintained at 37°C using an  
156 electronic heating pad. The cornea was protected using Lacri-Lube eye ointment.

157 **Intracisternal injections**

158 The mouse was placed prone on a stereotaxic frame and head-restrained with ear  
159 bars after the area between the head and shoulders was shaved. Under a dissection  
160 microscope, a 10 mm midsagittal incision of the skin was made inferior to the  
161 occipital crest. To expose the dura covering the cisterna magna, the subcutaneous  
162 tissue and occipital muscles (biventer cervicis and rectus capitis dorsalis) were  
163 separated using blunt-ended forceps and the posterior atlanto-occipital membrane  
164 was incised. Using a cotton swab, the area was treated with a cotton bud  
165 impregnated with viscous glycerol to help prevent CSF reflux. A glass capillary  
166 micropipette (Sigma, UK) with an adjusted diameter (of < 50 µm, made using a  
167 Sutter P97 Flaming Brown Pipette puller) was positioned perpendicular to the ear  
168 bars and advanced gently to penetrate the dura until resistance was overcome  
169 indicating entry into the cisterna magna. The capillary had been loaded with 2 µl of  
170 100 µM Aβ1-40 Hylite Fluor 555 (Bioscience), which was injected over 2.5 minutes at  
171 a rate of 0.8 µlmin<sup>-1</sup>. The microcapillary was left in situ for 2 minutes to prevent reflux  
172 and mice were culled 5 minutes or 30 minutes after withdrawal of the glass capillary  
173 through overdose with pentobarbital (200 mgkg<sup>-1</sup>). Mice were intracardially perfused  
174 with 0.01M phosphate buffer saline (PBS) followed by 4% paraformaldehyde (PFA)

175 in 0.01M PBS at a rate of 5 mlmin<sup>-1</sup>. Brains were dissected from the skull, post-fixed  
176 in 4 % PFA for 6-7 hours and cryoprotected with 30% sucrose in 0.01 M PBS for 48  
177 hours. The brains were sectioned into 20 µm thick coronal slices using a cryostat and  
178 stored at -20 °C.

### 179 **Double-labeling immunofluorescence**

180 For double labelling immunohistochemistry, tissue sections were incubated overnight  
181 with anti- $\alpha$ -smooth muscle actin (SMA) FITC (1:200, Sigma-Aldrich, Dorset, UK) for  
182 the identification of arteries. Anti-collagen IV (1:400, ABCAM, Cambridge, UK) was  
183 used to mark the basement membranes of blood vessels (Thermo Fisher Scientific,  
184 Paisley, UK). Brain sections were also incubated with rat monoclonal anti- $\alpha$ -2 laminin  
185 (1:200) to identify the astrocyte basement membranes of the glia limitans abutting  
186 the outer aspect of cortical arteries [13] or mouse monoclonal anti-GFAP (1:100) or  
187 polyclonal rabbit anti-CD163 (1:100) at 4 °C for 24 hr in a moist chamber. All primary  
188 antibodies were diluted in 0.1% PBST. Subsequently sections were incubated with  
189 the appropriate secondary antibodies conjugated to Alexafluor fluorophores.  
190 Photomicrographs of triple labelling immunohistochemistry were captured across the  
191 brain starting anterior from the olfactory bulbs moving posteriorly towards the  
192 cerebellum. Sections were analyzed using an SP8 confocal laser-scanning  
193 microscope (Milton Keys, UK) and exported to Image J software. Montages were  
194 created with Photoshop CS6.

### 195 **Cerebral blood vessel classification**

196 Arteries were differentiated from veins using an SMA marker, which only stains the  
197 smooth muscle cells that are present in arteries and arterioles. Vessels that were  
198 negative for SMA and had a diameter < 10 µm were classified as capillaries.

### 199 **Quantitative assessment of A $\beta$ -positive blood vessels**

200 To compare the depth of tracer 5 minutes and 30 minutes post-intracerebral injection  
201 in young and old mice, the distance of the A $\beta$ -positive blood arteries from the surface  
202 or base of the brain was measured by drawing two perpendicular lines (one travelling  
203 in the direction of the vessel and a tangent of the surface/base of the brain; see  
204 Online Resource 2) and determining the distance of the vessel from the point at  
205 which the two lines meet. A total of 108 full coronal sections were analyzed in 6 – 10  
206 week old mice (n = 3 per time point) and 56 sections in 24–30 month old mice (n = 3  
207 per time point) and all the A $\beta$ -positive blood SMA-positive arteries were quantified in  
208 this way. The sections quantified were taken at the level of the olfactory bulbs,  
209 cortex, ventricles, hippocampus, midbrain and cerebellum. The total length of each  
210 region (e.g. olfactory bulbs) was 180 µm.

### 211 **Statistical analysis**

212 The average of all distances in each brain region per mouse were used for statistics  
213 (n=3/group). Data were checked for normality using the D'Agostino & Pearson  
214 omnibus and Shapiro-Wilk normality tests. As the data in some groups were not  
215 normally distributed, all values were Log<sub>10</sub> transformed to obtain a normal  
216 distribution. One-way analysis of variance (ANOVA) with Sidak's post-hoc test was

217 used to compare the distance at which A $\beta$  was seen from the reference point at the  
218 surface of the brain within the same brain region at 5 and 30 minutes after  
219 intracisternal injections. Two-way ANOVA with Sidak's post-hoc test was used to  
220 compare the distance at which A $\beta$  was seen from the reference point at the surface  
221 of the brain between young and old mice at 5 and 30 minutes after intracisternal  
222 injections. Statistical analyses were performed using log-transformed data, with  
223 corresponding p-values indicated on graphs that were generated using non-  
224 transformed data.

225

## 226 **Results:**

### 227 ***Anatomical distribution of $\beta$ -amyloid after its injection into cisternal CSF***

228 First, the possible route of entry of A $\beta$ 1-40 (referred to from here as A $\beta$ ) contained  
229 within the CSF into the brain of 6–10 week old mice was evaluated by double-  
230 labelling immunohistochemistry and confocal microscopy. The anatomical distribution  
231 of A $\beta$  in the brain and the type of A $\beta$ -positive blood vessels were determined by  
232 staining the sections with an SMA marker to differentiate arteries from veins, a  
233 general basement membrane marker (collagen IV) and a specific astrocytic  
234 basement membrane marker ( $\alpha$ -2 laminin). The anatomical compartment in which  
235 the tracer was contained was defined and compared after 5 and 30 minutes of  
236 injection of tracer into the cisterna magna.

#### 237 6–10 week old mice, 5 minutes post-injection.

238 A $\beta$  was detected within the walls of leptomenigeal and cortical arteries (Figure 1).  
239 Immunocytochemistry with multiple labelling of collagen IV,  $\alpha$ -2 laminin and A $\beta$  tracer  
240 confirms the presence of A $\beta$  tracer in the brain disposed along pial-glia basement  
241 membranes on the outer aspects of arteries. Figure 1a shows a blood vessel  
242 penetrating the cerebral cortex with A $\beta$  tracer, stained red, in the vessel wall. Co-  
243 localisation of A $\beta$  tracer and  $\alpha$ -2 laminin in the pial-glia basement membrane is  
244 shown as yellow. Co-localisation of A $\beta$  tracer and collagen IV in the artery wall is  
245 depicted as fuchsia-pink. At higher magnification in figure 1b,  $\alpha$ -2 laminin in the  
246 astrocyte basement membranes of the glia limitans on the surface of the brain is  
247 stained green and co-localisation of A $\beta$  and  $\alpha$ -2 laminin wall of the artery is shown as  
248 yellow. Confirmation that the A $\beta$  tracer is in basement membranes on the outer  
249 aspect of arteries 5 min after injection into the CSF is seen in figure 1c. The blood  
250 vessel in longitudinal view is identified as an artery by the presence of smooth  
251 muscle cells stained green for smooth muscle actin in its wall. A $\beta$  tracer colocalizes  
252 with collagen IV (blue) as a fuchsia pink colour in a single fine layer of basement  
253 membrane on the outer aspects of the artery. This corresponds to the position on the  
254 outer aspect of the artery to the pial-glia basement membrane [24].

#### 255 6–10 week old mice, 30 minutes post-injection.

256 A $\beta$  was detected in the basement membranes surrounding smooth muscle cells  
257 within the walls of leptomenigeal and cortical arteries but not in the walls of  
258 capillaries and veins. The vessel in longitudinal view in figure 1d is an artery

259 identified by the smooth muscle cells in its wall stained green by  $\alpha$  smooth muscle  
260 cell actin (Figures 1d, 1f, 1j). At 30 min after injection into the cisterna magna, A $\beta$   
261 tracer (Fig 1e, 1k) is seen in a spiral configuration that represents the smooth  
262 muscle cell basement membranes within the artery wall; the fuchsia-pink staining  
263 (Fig 1d, 1i) represents co-localisation of A $\beta$  tracer in the walls of arteries in figure 1e,  
264 1k and collagen IV in the smooth muscle cell basement membranes (Fig 1g, 1j, 1l).  
265 In a single optical section from an arteriole, fuchsia pink co-localisation of collagen IV  
266 and A $\beta$  is seen running between green-stained smooth muscle cells in the tunica  
267 media of the arteriole (Fig 1h).

#### 268 24–30 month old mice, 5 minutes post-injection

269 At 5 min following injection of A $\beta$  tracer into the cisterna magna, the distribution of  
270 tracer is similar in the 24-30 month old mice to that found in the young 6-10 week old  
271 mice. A $\beta$  tracer was observed in the walls of arterioles, as depicted by  
272 immunostaining for green smooth muscle actin in Figures 2 a, b and in the walls of  
273 capillaries, as shown in Figure 2c. In Figure 2d, a blood vessel penetrating the  
274 surface of the cerebral cortex shows A $\beta$  tracer within the vessel wall and co-  
275 localizing with  $\alpha$ -2 laminin indicating its presence in the pial glial basement  
276 membrane on the abluminal aspect of the vessel. At higher magnification, in a single  
277 channel image in Figure 2e-f,  $\alpha$ -2 laminin in the glia limitans on the surface of the  
278 brain is stained green. Co-localisation of  $\alpha$ -2 laminin and A $\beta$  tracer in the pial-glial  
279 basement membrane on the outer aspect of the vessel wall is depicted in yellow.

#### 280 24–30 month old mice, 30 minutes post-injection

281 The pattern of distribution of A $\beta$  tracer in the walls of blood vessels in the older mice  
282 at 30 min after intracisternal injection is slightly different from that in the young mice.  
283 With regard to the arteries, the distribution of A $\beta$  tracer is the same in the two age  
284 groups. Figure 3a shows an artery and vein at the surface of the cerebral cortex. The  
285 artery is identified by the staining of smooth muscle cells in its wall; A $\beta$  is present in  
286 the same spiral pattern as smooth muscle cell basement membranes in the tunica  
287 media. A leptomenigeal artery in Figure 3 a,b shows the corresponding spiral  
288 pattern of smooth muscle cells in the tunica media. A $\beta$  tracer is present in a short  
289 region of the wall of a vein near the subarachnoid space in Figure 3a. A $\beta$  tracer, red,  
290 colocalizes with cells stained green for the macrophage marker CD 163 (Figure 3c).  
291 In addition, A $\beta$  tracer co-localizes with glial fibrillary acidic protein (GFAP) in  
292 perivascular astrocyte processes in Figure 3d.

#### 293 ***Periarterial penetration of $\beta$ -amyloid tracer into the brain parenchyma***

294 Next, the periarterial distances of A $\beta$  from the surface of the brain at 5 and 30  
295 minutes after intracisternal injection were determined using the quantification method  
296 illustrated in Online resource 1. Normally distributed data presented in the form of  
297 histograms show the Log<sub>10</sub> values.

#### 298 **Regional differences in distance of periarterial penetration of A $\beta$ into the** 299 **parenchyma after 5 minutes in 6–10 week old mice**

300 Soluble A $\beta$  injected into the CSF was only observed along the walls of

301 leptomeningeal and cortical arteries after 5 and 30 minutes of injection. No A $\beta$  was  
302 observed in the walls of capillaries or veins. The depth of penetration of A $\beta$  along the  
303 walls of cortical arteries was calculated in eleven different brain regions. At 5 min  
304 post-injection, there was no statistically significant difference between the periarterial  
305 A $\beta$  distance in the olfactory bulbs and the frontal, parietal, and entorhinal cortices.  
306 However, the distance at which A $\beta$  was detected in the walls of arteries was  
307 significantly greater in the visual cortex, caudoputamen, thalamus, pons and  
308 cerebellar molecular layer compared to the olfactory bulbs ( $P < 0.0001$ ). The greatest  
309 distance at which A $\beta$  was detected from the surface of the brain was 253.18 $\mu$ m and  
310 this was observed in the pons. No A $\beta$  was detected in the corpus callosum.

311 **Regional differences in the distance of periarterial penetration of A $\beta$  after 30**  
312 **minutes in 6–10 week old mice.**

313 Regional differences in the depth from the brain surface at which A $\beta$  within the walls  
314 of arteries was located in the parenchyma at 30 min from the intracisternal injection,  
315 were largely similar to those detected after 5 min. The main differences were in  
316 greater depths of penetration in the olfactory bulbs and the cortical, subcortical and  
317 posterior brain regions. There was a statistically significant difference in the distance  
318 at which periarterial A $\beta$  was detected within the parenchymal arteries in all eleven  
319 regions compared to the olfactory bulbs ( $P \leq 0.0001$ ), Fig 4.

320 **Regional differences in the periarterial distance of A $\beta$  penetration into the**  
321 **parenchyma in 24 – 30 month old mice**

322 After 5 minutes of injection into the cisterna magna of 24 – 30 month old mice, the  
323 greatest periarterial distance along which A $\beta$  was detected was in the pons and the  
324 least was detected in the thalamus. The periarterial A $\beta$  distance in the olfactory bulbs  
325 was significantly greater than the frontal cortex and the thalamus, but significantly  
326 less than the caudoputamen, tectum/tegmentum and pons ( $P < 0.0001$ ). The  
327 periarterial A $\beta$  distance in the caudoputamen was significantly higher than in the  
328 frontal cortex, thalamus and tectum/tegmentum.

329 At 30 minutes, the greatest periarterial distance at which A $\beta$  was observed in the  
330 parenchyma was no longer in the pons but in the caudoputamen, followed by the  
331 pons. Similar to the young mice, the periarterial distance of A $\beta$  was significantly  
332 greater after 30 min compared to 5 min in all of the brain regions analysed including  
333 the olfactory bulbs, frontal cortex, caudoputamen, thalamus, tectum/tegmentum and  
334 pons (one-way ANOVA,  $P < 0.0001$ ), Fig 5.

335 The comparison between the patterns of the periarterial distance of A $\beta$  entry from the  
336 CSF into the parenchyma at 5 and 30 minutes after intracisternal injection for both  
337 young and old mice is presented in Online Resource 3.

338 **Discussion:**

339 The first two major objectives in the present study were: (1) to demonstrate by  
340 immunocytochemistry that the pial-glial basement membranes are the entry route  
341 into the brain for soluble tracers from the CSF and (2) to test the hypothesis that  
342 tracers entering the brain from the CSF drain out of the brain parenchyma along the

343 IPAD pathways that are lymphatic drainage pathways from the brain for the  
344 elimination of fluid and solutes.

345 To fulfil these objectives, we performed multi-labelling immunocytochemistry and  
346 confocal microscope studies on young 6-10 week old mice and on aged 24-30 month  
347 old mice, both at two separate time points of 5 and 30 mins after injection of A $\beta$   
348 tracer into the CSF of the cisterna magna.

349 Our study showed similar but not exactly identical results in mice in the two age  
350 groups. We confirmed by immunocytochemistry and confocal microscopy our  
351 previous electron microscope studies that, within 5 minutes of injection into the CSF,  
352 tracer were present in the brain within basement membranes on the outer aspects of  
353 cortical artery walls. More exactly, the electron microscope study [24] and the  
354 present results using immunocytochemistry for  $\alpha$ -2 laminin [9] identified tracer in pial-  
355 glial basement membranes. These results suggest that one pathway for entry of  
356 tracers into the brain from the CSF is along the pial-glial basement membranes  
357 between the layer of pia mater and astrocytes in the perivascular glia limitans (figure  
358 6). This entry pathway was observed in the young and in aged mice.

359 Basement membranes and cell components surrounding cortical arteries are  
360 compacted so that there is no perivascular "space" for transport of tracers [23, 37];  
361 transport appears to be along basement membranes as shown in the present study.  
362 This contradicts the statement in the glymphatic literature that there is transport of  
363 tracers into the brain along perivascular "spaces" [17]. These authors used low  
364 resolution two-photon microscopy which did not resolve the microanatomy of the  
365 perivascular compartment. Furthermore, the subarachnoid space appears to have  
366 been mistaken for perivascular space in the electron micrographs [17].

367 At 30 mins following injection into the CSF of the cisterna magna, in the present  
368 study, A $\beta$  tracer co-localised with collagen IV in basement membranes within the  
369 walls of arteries. These basement membranes are in the position of smooth muscle  
370 cell basement membranes in the tunica media of arteries [4, 14, 27, 29] and  
371 correspond to the Intramural Peri-Arterial Drainage (IPAD) pathways that are the  
372 proposed route of drainage of interstitial fluid and solutes from the brain.

373 The pattern of distribution of A $\beta$  tracer in the artery wall at 30 minutes after injection  
374 into cisternal CSF was similar in the young 6-10 week and the old 24-30 month old  
375 mice. A $\beta$  tracer was located in the spirally arranged smooth muscle cell basement  
376 membranes within the tunica media of arteries within the cerebral cortex. This is the  
377 same IPAD pathway identified previously by intracerebral injections of tracer in mice  
378 and the same IPAD pathway in which the A $\beta$  is deposited in CAA [5, 19, 29]. Electron  
379 microscope studies of CAA have shown that fibrillary A $\beta$  is initially deposited in the  
380 lamina densa that forms the junction zone between basement membranes of  
381 adjacent smooth muscle cells in the tunica media [12, 38].

382 With the increase in volume of deposited A $\beta$  in CAA, the mass of A $\beta$  separates the  
383 basement membranes of adjacent smooth muscle cells [5, 19]. Although adjacent  
384 basement membranes are fused at the lamina densa in a normal artery, it appears  
385 that the two parts of the basement membrane can be separated by the deposition of  
386 amyloid [12]. Nevertheless, co-localisation of tracer with laminin in previous studies

387 [4] and collagen IV in the present study suggest that bulk flow of tracers, therefore of  
388 ISF and other solutes, out of the brain is along basement membranes that form the  
389 IPAD pathways.

390 The results of the present investigation suggest a possible route for connection  
391 between the inflow of tracers from the CSF along pial-glial basement membranes  
392 and the outflow along smooth muscle cell basement membranes in the IPAD  
393 pathway. In the older 24-30 month old mice, A $\beta$  tracer injected into the CSF was  
394 located within astrocytes and in macrophages in the brain parenchyma at 30  
395 minutes. This suggests that tracer had entered the extracellular, ISF compartment of  
396 the brain and been taken up by these cells. Furthermore, A $\beta$  tracer was located in the  
397 walls of brain capillaries associated with collagen IV in the capillary basement  
398 membranes. It seems most probable that the A $\beta$  tracer drains out of the brain initially  
399 along basement membranes in the walls of cerebral capillaries and then along  
400 smooth muscle cell basement membranes in the walls of cerebral arterioles and  
401 arteries. **This is effectively the same IPAD pathway identified for the outflow of**  
402 **tracers injected directly into the brain parenchyma [4]**

403 Previous studies have suggested that tracers entering the brain from the CSF drain  
404 out of the brain along the walls of veins [17]. This suggestion is derived not from  
405 injection of tracers into the CSF but from intracerebral injections of tracer. Veins were  
406 not conclusively identified in these studies, and it is unclear whether the tracer was  
407 even present the walls of blood vessels or in the surrounding brain tissue. In Iliff et al  
408 [17] the veins were identified by the absence of NG2Ds-Red rather than  
409 immunocytochemistry for the absence of smooth muscle actin [17]. Recent studies  
410 demonstrate that NG2Ds-Red is not specific for identification of arteries, so it is  
411 possible that some of the vessels that were NG2-DsRed negative may indeed have  
412 been smooth muscle actin positive arterioles [15].

413 It is also likely that in this study [17] tracer leaked from the brain into the CSF during  
414 the intracerebral injections due to the use of a large 33G needle for injecting a large  
415 1 $\mu$ l volume of tracer. This would account for the appearance of tracer as oval  
416 patches resembling macrophages surrounding veins in the subarachnoid space.  
417 Furthermore, the time of examination of the brain was one hour in **ref 20** rather than  
418 the much earlier time of 5min at which it has been shown that tracers, injected  
419 intracerebrally, drain out of the brain along IPAD pathways [4]. In the present study,  
420 tracer was only rarely detected in the walls of veins **for short distances very** near the  
421 surface of the brain and this probably represented incursion of tracer from the  
422 subarachnoid space. For example, the vein in Fig 3a shows a small amount of A $\beta$   
423 (red) in its wall near the surface of the brain but no A $\beta$  in the wall further into the  
424 brain. This short ingress of tracer into the brain from the SAS along veins has been  
425 recorded in [17] and recent studies [1, 13, 27].

426 Other recent studies cast doubt upon the circulation of A $\beta$  from the periarterial  
427 convective influx compartment to the perivenous compartment for clearance into the  
428 CSF [34, 35]. Our results support the convective influx of A $\beta$  along arterial  
429 perivascular compartments in the pial-glial basement membranes, but we did not  
430 observe perivenous clearance into the CSF. This field of work is significant not only  
431 for the pathogenesis of CAA, but also for the distribution of drugs into the

432 parenchyma after intrathecal delivery, as well as for the interpretation of biomarkers  
433 in the CSF.

434 The third objective of the present study was to determine the range of depths of  
435 penetration of tracer alongside arteries in different regions of the brain at the time  
436 points of 5 and 30 min in young and aged mice. We demonstrated that the pons is  
437 the region with the highest penetration of A $\beta$  at both ages at 5 minutes after  
438 intracisternal injection. Recently we showed in vivo that entry of contrast agent is  
439 most efficient in the midbrain of dogs and the pial-glial basement membranes were  
440 also thickest in the midbrain [10]. This suggests that the brainstem is an area most  
441 efficiently reached by therapeutic agents from the CSF, most likely also explaining  
442 the success of intracisternally administered antisense oligonucleotides in the  
443 treatment of spinal muscular atrophy (SMA) [6, 21]. SPINRAZA is an anti-sense  
444 oligonucleotide that alters the splicing of Survival Motor Neuron (SMN) pre-  
445 messenger RNA in order to increase production of full-length normal SMN protein.  
446 Following a randomized, double-blind, sham-controlled study in infantile-onset SMA  
447 where SPINRAZA ([www.spinraza.com](http://www.spinraza.com)) was administered intrathecally, the motor  
448 milestones improved significantly and the numbers of deaths decreased. Our results  
449 suggest that it is possible for solutes to reach the neurons in the brainstem within 5  
450 minutes increasing thus the understanding of how anti-sense oligonucleotides that  
451 are in development for intrathecal administration in the treatment of neurological  
452 diseases may reach their targets [31].

453 Although in the present study the depth at which A $\beta$  was observed in the brain  
454 increased after 30 minutes, most was observed in the pial glial basement  
455 membranes of arteries. This suggests that therapeutic agents would need to then  
456 diffuse from the pial-glial basement membranes towards their target, reducing the  
457 concentration and therapeutic efficiency. Only 10–15% of the intrathecally  
458 administered dose of proteins in cynomolgus monkeys was observed within the  
459 parenchyma at 2.5h after injection of tracer into the CSF and by 24h this decreased  
460 to 2% [25].

461 The exact dynamics of biomarkers in the CSF associated with neuropathological  
462 conditions remain unclear. Although with advancement of Alzheimer's disease, there  
463 is a decrease in the amount of both A $\beta$ 1-40 and 1-42 in the CSF, there is a  
464 corresponding increase in total and phosphorylated forms of tau [16]. It is probable  
465 that the A $\beta$  becomes entrapped in the IPAD pathways as CAA and therefore less A $\beta$   
466 is able to reach the CSF; this is in contrast to the more soluble tau that may be able  
467 to filter more readily along the chains of glycoproteins and proteoglycan components  
468 of the basement membranes surrounding smooth muscle cells.

469 In conclusion, we suggest that the present observations support the working  
470 hypothesis that tracers injected into the CSF pass into the brain along pial-glial  
471 basement membranes on the outer aspects of cortical arteries, enter the brain  
472 parenchyma and drain out of the brain along pericapillary and periarterial basement  
473 membranes that form the IPAD pathway for the drainage of ISF and solutes from the  
474 brain. In older mice, this pathway is impaired, as by 30 minutes after intracisternal  
475 injection, the tracer is observed in the capillary basement membranes, as well as in  
476 astrocytes and macrophages.

**Figure legends:**

478 **Figure 1** - Anatomical entry route of A $\beta$  into the young adult brain from the CSF at 5  
 479 and 30 minutes post-injection. Young 6-10 week old mice: *Entry of amyloid- $\beta$  (A $\beta$ )*  
 480 *tracer into the brain from the CSF at 5 mins (a-c). Drainage of A $\beta$  tracer from the*  
 481 *brain along the walls of arteries at 30 mins (d-l).* (a) 5 mins: The surface of the  
 482 cerebral cortex (blue line) and a cortical artery passing into the brain with A $\beta$  tracer  
 483 red in its walls. A $\beta$  tracer colocalized with  $\alpha$ 2-laminin in the pial-glial basement  
 484 membrane (yellow) indicated by the white arrow. (b) 5 mins: A single optical section  
 485 of the artery enclosed in the box in (a) showing  $\alpha$ 2-laminin in the astrocyte basement  
 486 membrane of the glia limitans on the surface of the brain (green) and co-localisation  
 487 of A $\beta$  and  $\alpha$ 2-laminin in the pial-glial basement membrane on the outer aspect of the  
 488 wall of the artery (yellow) (white arrow); (c) 5mins: the profile of a cortical artery with  
 489 smooth muscle cells (green) in its wall shows A $\beta$  tracer (red) colocalized (pink) with  
 490 collagen IV (blue) in the pial basement membrane on the outer surface of the artery  
 491 (white arrows). *At 30 min after injection as shown in figures (d-l), the distribution of*  
 492 *the A $\beta$  in the artery walls is very different from that seen at 5 mins in figures (a-c).* (d)  
 493 An artery identified by green smooth muscle actin in its wall (f, j) shows A $\beta$  tracer  
 494 (red, e, k) colocalized (pink) with collagen IV (blue, g, l) within the wall of the artery in  
 495 a spiral or ladder-type distribution (arrows in d), closely resembling the pattern of  
 496 deposition of A $\beta$  in the walls of arteries as cerebral amyloid angiopathy (CAA); h) a  
 497 single optical section from the artery in d) showing the A $\beta$  tracer (red) between the  
 498 smooth muscle actin staining (green).

499 **Figure 2** - Anatomical entry route of A $\beta$  into old 24–30 month old mouse brain from  
 500 the CSF at 5 minutes post-injection: (a-c): Arteries showing A $\beta$  (red) along the walls  
 501 of arterioles of 10-20 $\mu$ m diameter labelled with collagen IV (blue) and smooth muscle  
 502 actin (green); (d) An artery entering the cerebral cortex (arrow) showing A $\beta$  (red)  
 503 extending into the brain. (e): Enlargement of the artery in (d) showing laminin  $\alpha$ -2  
 504 staining in the glia limitans on the surface of the brain (green) and co-localisation of  
 505 the amyloid with laminin  $\alpha$ -2 in the vessel wall (yellow) as indicated by the arrow. (f)  
 506 single optical section of artery in e); g) single channel image of laminin  $\alpha$ -2 from d); h)  
 507 single channel image of collagen IV from d) ; i) single channel image of A $\beta$  from d)

508 **Figure 3** - Anatomical route for drainage of A $\beta$  out of the brain following entry from  
 509 the CSF at 30 minutes post-injection in old 24-30 month mice: **(a)** An artery and vein  
 510 at the surface of the brain. The artery is identified by smooth muscle cells in its wall  
 511 (green). A $\beta$  tracer (red) is present in a ladder-like pattern in the wall of the artery. A $\beta$   
 512 (red) in the wall of a vein is only seen at the surface suggesting that the A $\beta$  here has  
 513 entered from the CSF and not drained from the brain. Only occasional veins had A $\beta$   
 514 in their walls. (b) Enlargement of the artery in (a) showing the ladder-like distribution  
 515 of A $\beta$  that resembles the distribution of amyloid in CAA [29]. At the surface of the  
 516 brain is a branch of a leptomenigeal artery showing the ladder-like distribution of  
 517 smooth muscle cells in the tunica media. The A $\beta$  is in the intramural periarterial  
 518 drainage (IPAD) pathway; c) Macrophages take up A $\beta$  tracer at 30 min after injection.  
 519 The arrows indicate A $\beta$  (red) within macrophages stained for the macrophage marker  
 520 CD163 (green); d) Astrocytes are stained for GFAP (green). Co-localisation (yellow)  
 521 of A $\beta$  and GFAP indicates uptake of A $\beta$  tracer by perivascular astrocytes.

522 **Figure 4** - Periarterial penetration of A $\beta$  is of greater distance after 30 minutes than  
523 after 5 minutes in cortical, subcortical and posterior brain regions of young mice. Bar  
524 charts of periarterial A $\beta$  distance against time after injection into cisternal CSF (5 and  
525 30 minutes) in the olfactory bulbs (a), somatomotor area (b), somatosensory area  
526 and caudoputamen (c), thalamus and hypothalamus (d), superior colliculus, pontine  
527 reticular nucleus, entorhinal and visual areas (e) and cerebellar molecular layer (f).  
528 Values are presented as mean  $\pm$  SEM of untransformed data, with p values indicated  
529 for log<sub>10</sub>-transformed data (one-way ANOVA with Sidak's post-hoc).

530 **Figure 5** - Regional differences in periarterial distance of penetration of A $\beta$  at 5 and  
531 30 minutes post-injection in old mice. (a) Schematic showing a sagittal mouse brain  
532 section with five brain levels (I – V) from which distance measurements were taken in  
533 6 brain regions at 5 minutes after injection of A $\beta$  into cisterna magna. ( Allen Institute  
534 for Brain Science. Allen Mouse Brain Atlas. Available from: [http://mouse.brain-  
535 map.org/static/atlas.](http://mouse.brain-map.org/static/atlas)) (b) Bar charts of periarterial A $\beta$  distance against time after  
536 injection into cisternal CSF (5 and 30 minutes) in the olfactory bulbs (teal),  
537 somatomotor area (green), caudoputamen (blue), thalamus (salmon), superior  
538 colliculus (pink) and pontine reticular nucleus (orange). Values are presented as  
539 mean  $\pm$  SEM of untransformed data, with p values indicated for log<sub>10</sub>-transformed  
540 data (one-way ANOVA with Sidak's post-hoc).

541 **Figure 6** - Pathways for influx of CSF into the brain and drainage of CSF/ISF out of  
542 the brain along capillary and periarterial basement membranes. (1) Entry of tracers  
543 from the CSF into the brain along pial-glia basement membranes on the outer  
544 aspects of artery walls. The sites of entry of tracer into the brain extracellular  
545 compartment are unclear and could be multiple. (2) CSF enters the brain  
546 parenchyma and (3) mixes with interstitial fluid (ISF). (4) The mixture of CSF/ISF  
547 diffuses through the narrow extracellular spaces of the brain to enter (5) basement  
548 membranes in the walls of capillaries to drain out of the brain along (6) basement  
549 membranes of smooth muscle cells in the tunica media in the walls of arterioles and  
550 arteries (IPAD pathway).

551 **Key to the Microanatomy of the capillary and artery walls:** **BM1:** endothelial  
552 basement membrane. **BM2:** smooth muscle cell basement membrane identified in  
553 this study by the presence of collagen IV. **BM3:** basement membrane between pia  
554 mater (pink) and smooth muscle cell. **BM4:** pia-glia basement membrane between  
555 the pia mater and the astrocytes of the glia limitans. In this study BM4 is identified by  
556 the presence of  $\alpha$ 2-laminin [9, 13]. **Proposed route of IPAD:** Tracer is located in the  
557 capillary endothelial basement membrane (5) apparently entering from the brain  
558 parenchyma. In the artery wall, tracer is observed in the basement membranes  
559 between smooth muscle cells (light purple) but not in the basement membranes on  
560 the outer aspect of the artery wall or in the endothelial basement membrane of the  
561 artery wall (both dull blue) [4, 27]. The light green arrow indicates the proposed  
562 Intramural Peri-Arterial Drainage (IPAD) pathway for fluid and solutes out of the  
563 brain.

564

565

566 **Online Resource legends:**

567 Online Resource 1- Male C57BL/6 mice 10 weeks old (n=3) were anaesthetised  
568 either with isoflurane (1% with 0.8 litre/min O<sup>2</sup>) or with 10mg/ml ketamine & 1mg/ml  
569 xylazine. The oxygen saturation, heart and breathing rates were recorded for 10  
570 minutes using a non-invasive infrared thigh sensor attached to a MouseOx Plus  
571 Oximeter running premium software (STARR Life Sciences, Holliston, Ma, USA). The  
572 isoflurane maintained the heart rate and oxygen pressure at physiological levels  
573 when compared to ketamine&xylazine.

574

575 Online Resource 2 - Method for measuring distance of periarterial A $\beta$  penetration into  
576 the brain. (a) Sagittal view of mouse brain illustrating the locations (I – VI) at which  
577 representative slices were taken to analyse the penetration of A $\beta$  in the brain from  
578 the CSF. (© 2018 Allen Institute for Brain Science. Allen Mouse Brain Atlas.  
579 Available from: [http://mouse.brain-map.org/static/atlas.](http://mouse.brain-map.org/static/atlas)) (A, I-VI) Sections were  
580 taken from the level of the olfactory bulbs, cerebral cortex, lateral ventricles, anterior  
581 hippocampus, midbrain/hindbrain and cerebellum. The total length of each level  
582 analysed per mouse (n = 3/group) was 180  $\mu$ m (double headed arrow). (b) Coronal  
583 view of the brain levels selected for analysis; mouse brains for this study were  
584 sectioned coronally. (c) Confocal micrographs corresponding with the boxes in B, III  
585 (1-3). (c, 1) Micrograph illustrating two perpendicular lines, a tangent to the midline  
586 fissure in the cerebral and another line in the direction of the A $\beta$ -positive vessel. (c,  
587 2) Same quantification method applied to the A $\beta$ -positive vessel in the  
588 caudoputamen in relation to the lateral ventricle (asterisk). (c, 3) Distance of A $\beta$ -  
589 positive vessel measured in the striatum in relation to the base of the brain. Scale  
590 bar: 150  $\mu$ m.

591 Online Resource 3 - Distance of periarterial A $\beta$  penetration into the brain in young  
592 and old mice at 5 and 30 mins post-injection. Bar charts of periarterial A $\beta$  distance  
593 against time after injection into cisternal CSF (5 and 30 minutes) in the olfactory  
594 bulbs (a), somatomotor area (b), caudoputamen (c), thalamus (d), superior colliculus  
595 (e) and pontine reticular nucleus (f) of young and old mice. Values are presented as  
596 mean  $\pm$  SEM of untransformed data, with p values indicated for log<sub>10</sub>-transformed  
597 data (two-way ANOVA with Sidak's posthoc).

**References:**

- 599 1 Abbott NJ, Pizzo ME, Preston JE, Janigro D, Thorne RG (2018) The role of  
600 brain barriers in fluid movement in the CNS: is there a 'glymphatic' system?  
601 *Acta neuropathologica* 135: 387-407 Doi 10.1007/s00401-018-1812-4
- 602 2 Arbel-Ornath M, Hudry E, Eikermann-Haerter K, Hou S, Gregory JL, Zhao L,  
603 Betensky RA, Frosch MP, Greenberg SM, Bacskai BJ (2013) Interstitial fluid  
604 drainage is impaired in ischemic stroke and Alzheimer's disease mouse  
605 models. *Acta neuropathologica*: Doi 10.1007/s00401-013-1145-2
- 606 3 Aspelund A, Antila S, Proulx ST, Karlisen TV, Karaman S, Detmar M, Wiig H,  
607 Alitalo K (2015) A dural lymphatic vascular system that drains brain interstitial  
608 fluid and macromolecules. *The Journal of experimental medicine* 212: 991-  
609 999 Doi 10.1084/jem.20142290
- 610 4 Carare RO, Bernardes-Silva M, Newman TA, Page AM, Nicoll JA, Perry VH,  
611 Weller RO (2008) Solutes, but not cells, drain from the brain parenchyma  
612 along basement membranes of capillaries and arteries: significance for  
613 cerebral amyloid angiopathy and neuroimmunology.  
614 *NeuropatholApplNeurobiol* 34: 131-144
- 615 5 Carare RO, Hawkes CA, Jeffrey M, Kalaria RN, Weller RO (2013) Review:  
616 cerebral amyloid angiopathy, prion angiopathy, CADASIL and the spectrum of  
617 protein elimination failure angiopathies (PEFA) in neurodegenerative disease  
618 with a focus on therapy. *Neuropathology and applied neurobiology* 39: 593-  
619 611 Doi 10.1111/nan.12042
- 620 6 Chiriboga CA, Swoboda KJ, Darras BT, Iannaccone ST, Montes J, De Vivo  
621 DC, Norris DA, Bennett CF, Bishop KM (2016) Results from a phase 1 study  
622 of nusinersen (ISIS-SMN(Rx)) in children with spinal muscular atrophy.  
623 *Neurology* 86: 890-897 Doi 10.1212/WNL.0000000000002445
- 624 7 Clapham R, O'Sullivan E, Weller RO, Carare RO (2010) Cervical lymph  
625 nodes are found in direct relationship with the internal carotid artery:  
626 significance for the lymphatic drainage of the brain. *Clin Anat* 23: 43-47 Doi  
627 10.1002/ca.20887
- 628 8 Cserr HF, Knopf PM (1992) Cervical lymphatics, the blood-brain barrier and  
629 the immunoreactivity of the brain: a new view. *ImmunolToday* 13: 507-512
- 630 9 Di Russo J, Hannocks MJ, Luik AL, Song J, Zhang X, Yousif L, Aspate G,  
631 Hallmann R, Sorokin L (2017) Vascular laminins in physiology and pathology.  
632 *Matrix biology : journal of the International Society for Matrix Biology* 57-58:  
633 140-148 Doi 10.1016/j.matbio.2016.06.008
- 634 10 Dobson H, MacGregor Sharp M, Cumpsty R, Criswell TP, Wellman T,  
635 Finucane C, Sullivan JM, Weller RO, Verma A, Carare RO (2017) The  
636 perivascular pathways for influx of cerebrospinal fluid are most efficient in the  
637 midbrain. *Clin Sci (Lond)*: Doi 10.1042/CS20171265
- 638 11 Engelhardt B, Carare RO, Bechmann I, Flugel A, Laman JD, Weller RO  
639 (2016) Vascular, glial, and lymphatic immune gateways of the central nervous  
640 system. *Acta neuropathologica* 132: 317-338 Doi 10.1007/s00401-016-1606-  
641 5
- 642 12 Frackowiak J, Zoltowska A, Wisniewski HM (1994) Non-fibrillar beta-amyloid  
643 protein is associated with smooth muscle cells of vessel walls in Alzheimer  
644 disease. *Journal of neuropathology and experimental neurology* 53 637-645
- 645 13 Hannocks MJ, Pizzo ME, Huppert J, Despande T, Abbott NJ, Thorne RG,  
646 Sorokin L (2017) Molecular characterization of perivascular drainage  
647 pathways in the murine brain. *Journal of cerebral blood flow and metabolism :  
648 official journal of the International Society of Cerebral Blood Flow and  
649 Metabolism*: 271678X17749689 Doi 10.1177/0271678X17749689
- 650 14 Hawkes CA, Jayakody N, Johnston DA, Bechmann I, Carare RO (2014)  
651 Failure of Perivascular Drainage of beta-amyloid in Cerebral Amyloid  
652 Angiopathy. *Brain Pathol* 24: 396-403 Doi 10.1111/bpa.12159
- 653 15 He L, Vanlandewijck M, Raschperger E, Andaloussi Mae M, Jung B,  
654 Lebouvier T, Ando K, Hofmann J, Keller A, Betsholtz C (2016) Analysis of the

655 brain mural cell transcriptome. *Scientific reports* 6: 35108 Doi  
656 10.1038/srep35108

657 16 Hoglund K, Kern S, Zettergren A, Borjesson-Hansson A, Zetterberg H, Skoog  
658 I, Blennow K (2017) Preclinical amyloid pathology biomarker positivity: effects  
659 on tau pathology and neurodegeneration. *Translational psychiatry* 7: e995  
660 Doi 10.1038/tp.2016.252

661 17 Iliff JJ, Wang M, Liao Y, Plogg BA, Peng W, Gundersen GA, Benveniste H,  
662 Vates GE, Deane R, Goldman SA et al (2012) A Paravascular Pathway  
663 Facilitates CSF Flow Through the Brain Parenchyma and the Clearance of  
664 Interstitial Solutes, Including Amyloid beta. *Science translational medicine* 4:  
665 147ra111 Doi 10.1126/scitranslmed.3003748

666 18 Johnston M, Zakharov A, Papaiconomou C, Salmasi G, Armstrong D (2004)  
667 Evidence of connections between cerebrospinal fluid and nasal lymphatic  
668 vessels in humans, non-human primates and other mammalian species.  
669 *Cerebrospinal fluid research* 1: 2-15

670 19 Keable A, Fenna K, Yuen HM, Johnston DA, Smyth NR, Smith C, Al-Shahi  
671 Salman R, Samarasekera N, Nicoll JA, Attems J et al (2016) Deposition of  
672 amyloid beta in the walls of human leptomeningeal arteries in relation to  
673 perivascular drainage pathways in cerebral amyloid angiopathy. *Biochimica et*  
674 *biophysica acta* 1862: 1037-1046 Doi 10.1016/j.bbadis.2015.08.024

675 20 Kida S, Pantazis A, Weller RO (1993) CSF drains directly from the  
676 subarachnoid space into nasal lymphatics in the rat. *Anatomy, histology and*  
677 *immunological significance. Neuropathol Appl Neurobiol* 19: 480-488

678 21 Kolb SJ, Coffey CS, Yankey JW, Krossschell K, Arnold WD, Rutkove SB,  
679 Swoboda KJ, Reyna SP, Sakonju A, Darras BT et al (2016) Baseline results of  
680 the NeuroNEXT spinal muscular atrophy infant biomarker study. *Annals of*  
681 *clinical and translational neurology* 3: 132-145 Doi 10.1002/acn3.283

682 22 Louveau A, Smirnov I, Keyes TJ, Eccles JD, Rouhani SJ, Peske JD, Derecki  
683 NC, Castle D, Mandell JW, Lee K et al (2015) Structural and functional  
684 features of central nervous system lymphatic vessels. *Nature*: Doi  
685 10.1038/nature14432

686 23 MacGregor Sharp M, Bulters D, Brandner S, Holton J, Verma A, Werring DJ,  
687 Carare RO (2018) The fine anatomy of the perivascular compartment in the  
688 human brain: relevance to dilated perivascular spaces in cerebral amyloid  
689 angiopathy. *Neuropathology and applied neurobiology*: Doi  
690 10.1111/nan.12480

691 24 Morris AW, Sharp MM, Albargothy NJ, Fernandes R, Hawkes CA, Verma A,  
692 Weller RO, Carare RO (2016) Vascular basement membranes as pathways  
693 for the passage of fluid into and out of the brain. *Acta neuropathologica*: Doi  
694 10.1007/s00401-016-1555-z

695 25 Papisov MI, Belov VV, Gannon KS (2013) Physiology of the intrathecal bolus:  
696 the leptomeningeal route for macromolecule and particle delivery to CNS.  
697 *Molecular pharmaceuticals* 10: 1522-1532 Doi 10.1021/mp300474m

698 26 Pappolla M, Sambamurti K, Vidal R, Pacheco-Quinto J, Poeggeler B,  
699 Matsubara E (2014) Evidence for lymphatic Abeta clearance in Alzheimer's  
700 transgenic mice. *Neurobiology of disease* 71: 215-219 Doi  
701 10.1016/j.nbd.2014.07.012

702 27 Pizzo ME, Wolak DJ, Kumar NN, Brunette E, Brunnuquell CL, Hannocks MJ,  
703 Abbott NJ, Meyerand ME, Sorokin L, Stanimirovic DB et al (2017) Intrathecal  
704 antibody distribution in the rat brain: surface diffusion, perivascular transport,  
705 and osmotic enhancement of delivery. *The Journal of physiology*: Doi  
706 10.1113/JP275105

707 28 Pollock H, Hutchings M, Weller RO, Zhang ET (1997) Perivascular spaces in  
708 the basal ganglia of the human brain: their relationship to lacunes. *J Anat* 191  
709 ( Pt 3): 337-346

710 29 Preston SD, Steart PV, Wilkinson A, Nicoll JA, Weller RO (2003) Capillary  
711 and arterial cerebral amyloid angiopathy in Alzheimer's disease: defining the

712 perivascular route for the elimination of amyloid beta from the human brain.  
713 *NeuropatholAppl Neurobiol* 29: 106-117

714 30 Rennels ML, Gregory TF, Blaumanis OR, Fujimoto K, Grady PA (1985)  
715 Evidence for a 'paravascular' fluid circulation in the mammalian central  
716 nervous system, provided by the rapid distribution of tracer protein throughout  
717 the brain from the subarachnoid space. *Brain research* 326 47-63

718 31 Rinaldi C, Wood MJA (2018) Antisense oligonucleotides: the next frontier for  
719 treatment of neurological disorders. *Nature reviews Neurology* 14: 9-21 Doi  
720 10.1038/nrneurol.2017.148

721 32 Shams S, Martola J, Charidimou A, Larvie M, Granberg T, Shams M,  
722 Kristoffersen-Wiberg M, Wahlund LO (2017) Topography and Determinants of  
723 Magnetic Resonance Imaging (MRI)-Visible Perivascular Spaces in a Large  
724 Memory Clinic Cohort. *J Am Heart Assoc* 6: Doi 10.1161/JAHA.117.006279

725 33 Shinkai Y, Yoshimura M, Ito Y, Odaka A, Suzuki N, Yanagisawa K, Ihara Y  
726 (1995) Amyloid beta-proteins 1-40 and 1-42(43) in the soluble fraction of  
727 extra- and intracranial blood vessels. *Annals of neurology* 38 421-428

728 34 Smith AJ, Verkman AS (2017) The "glymphatic" mechanism for solute  
729 clearance in Alzheimer's disease: game changer or unproven speculation?  
730 *The FASEB journal : official publication of the Federation of American*  
731 *Societies for Experimental Biology*: Doi 10.1096/fj.201700999

732 35 Smith AJ, Yao X, Dix JA, Jin BJ, Verkman AS (2017) Test of the 'glymphatic'  
733 hypothesis demonstrates diffusive and aquaporin-4-independent solute  
734 transport in rodent brain parenchyma. *Elife* 6: Doi 10.7554/eLife.27679

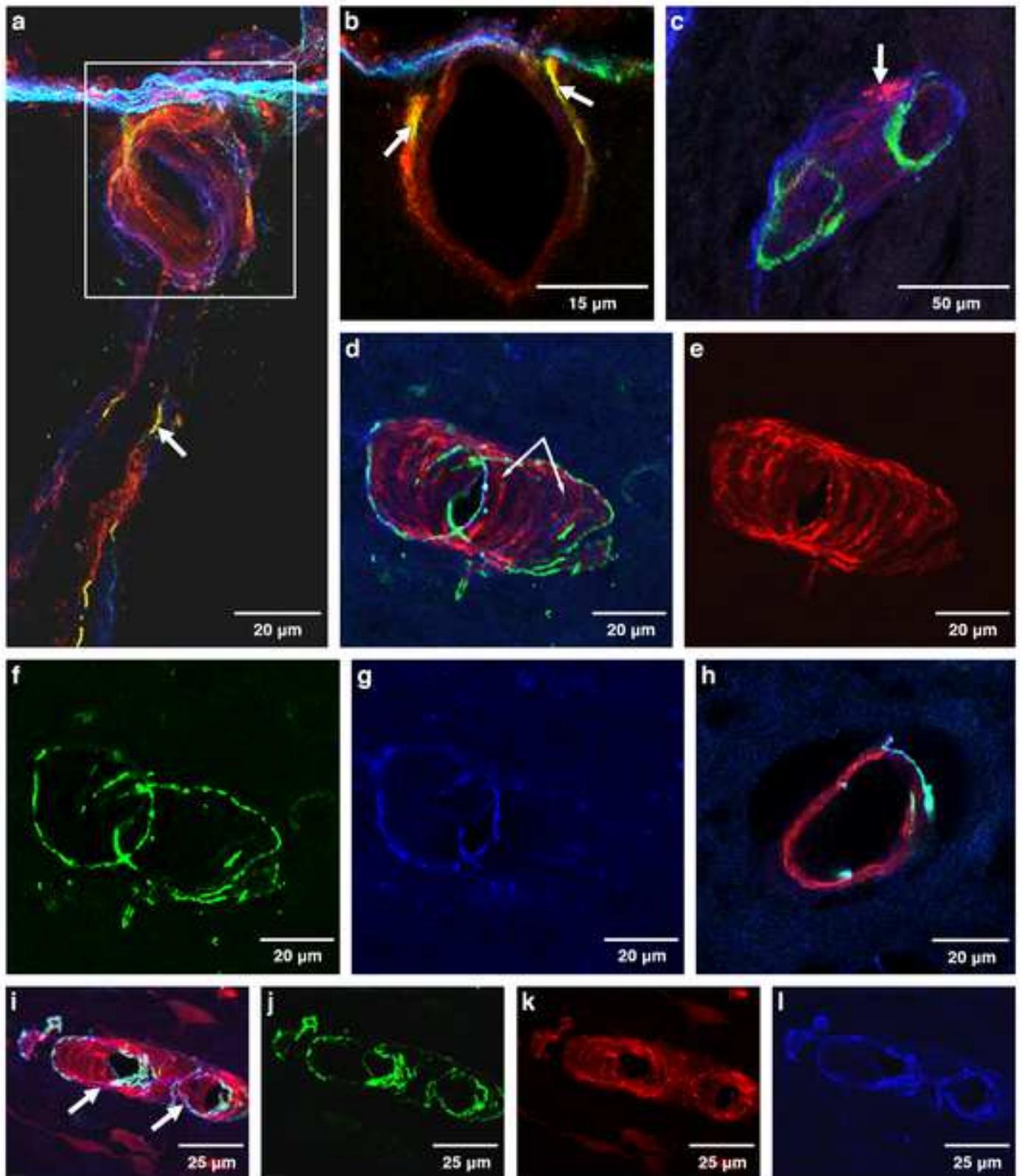
735 36 Szentistvanyi I, Patlak CS, Ellis RA, Cserr HF (1984) Drainage of interstitial  
736 fluid from different regions of rat brain *AmJ Physiol* 246: F835-F844

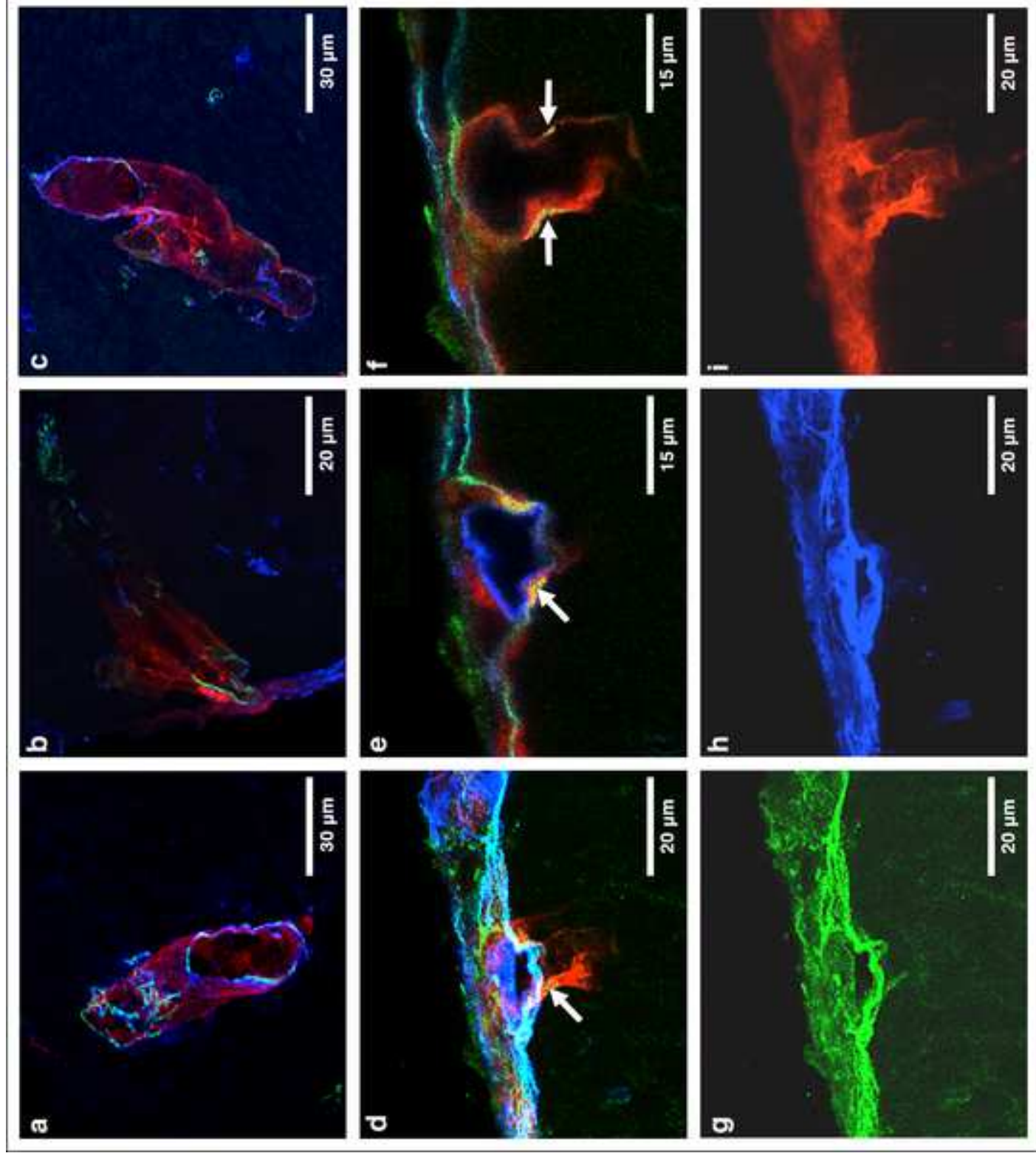
737 37 Weller RO, Sharp MM, Christodoulides M, Carare RO, Mollgard K (2018) The  
738 meninges as barriers and facilitators for the movement of fluid, cells and  
739 pathogens related to the rodent and human CNS. *Acta neuropathologica* 135:  
740 363-385 Doi 10.1007/s00401-018-1809-z

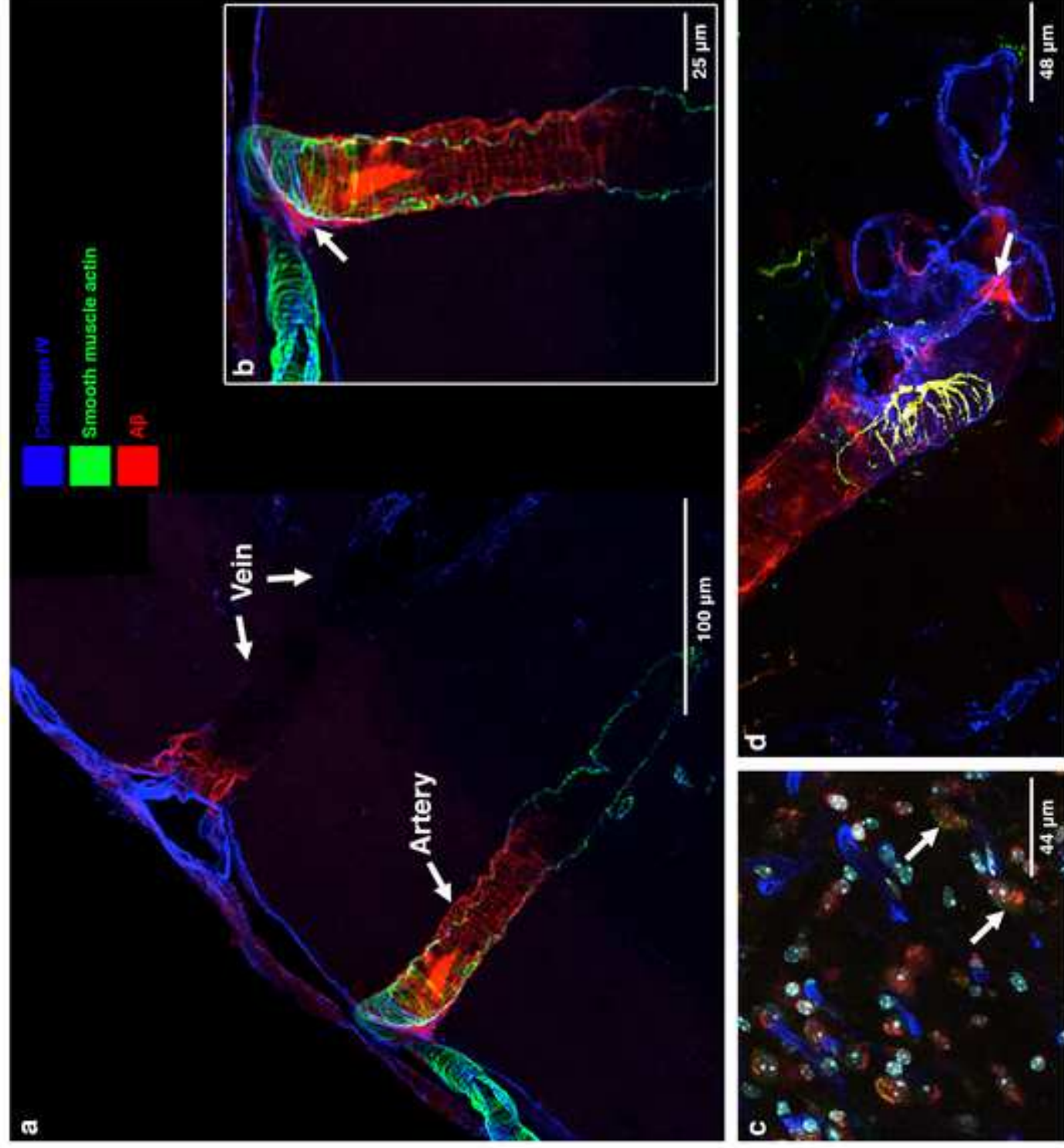
741 38 Wisniewski HM, Wegiel J (1994) Beta-amyloid formation by myocytes of  
742 leptomeningeal vessels. *Acta neuropathologica* 87: 233-241

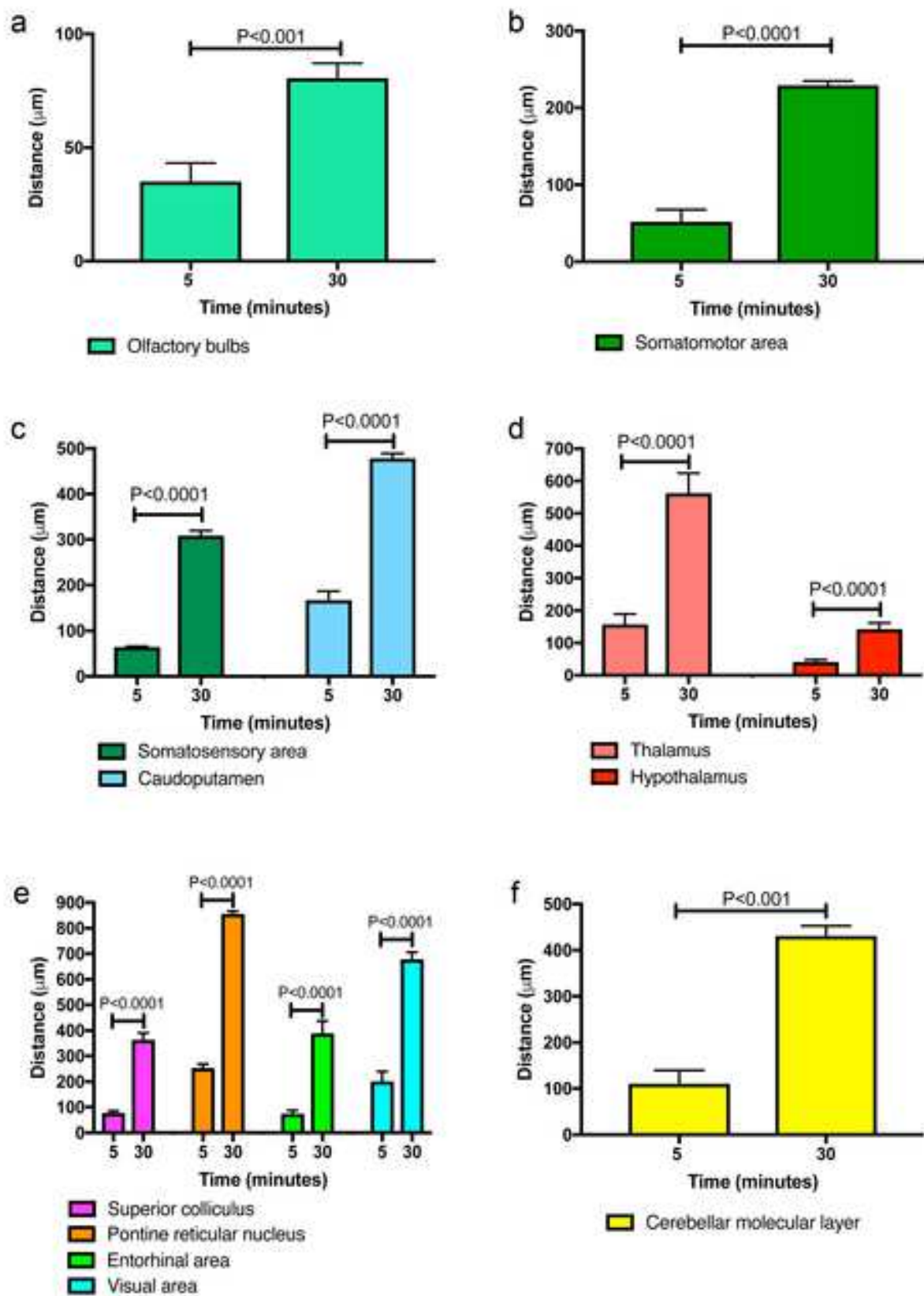
743 39 Yamada S, dePasquale M, Patlak CS, Cserr HF (1991) Albumin outflow into  
744 deep cervical lymph from different regions of rabbit brain. *American journal of*  
745 *physiology* 261: H1197-H1204

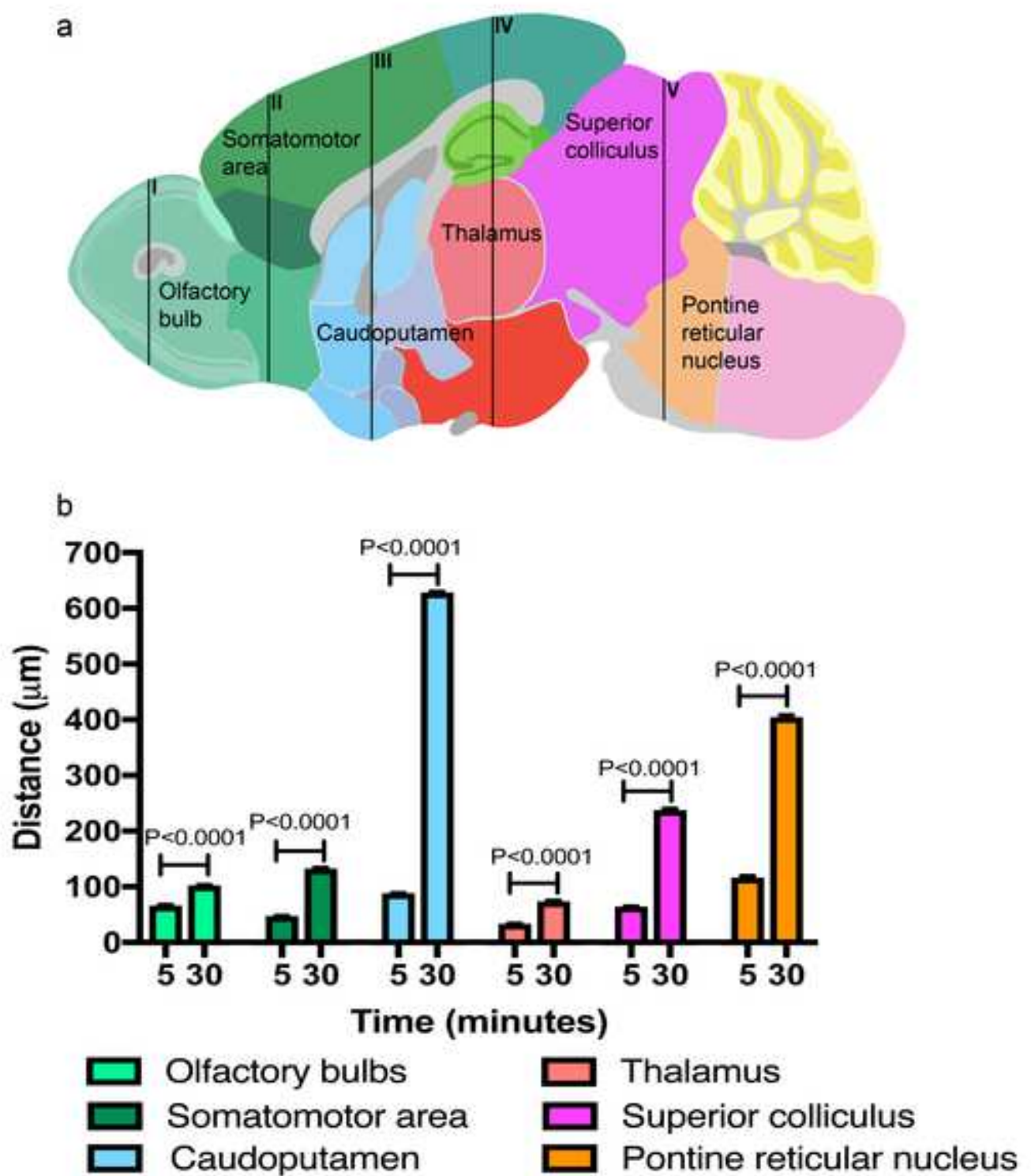
746 40 Zhang ET, Inman CB, Weller RO (1990) Interrelationships of the pia mater  
747 and the perivascular (Virchow-Robin) spaces in the human cerebrum. *J Anat*  
748 170: 111-123  
749

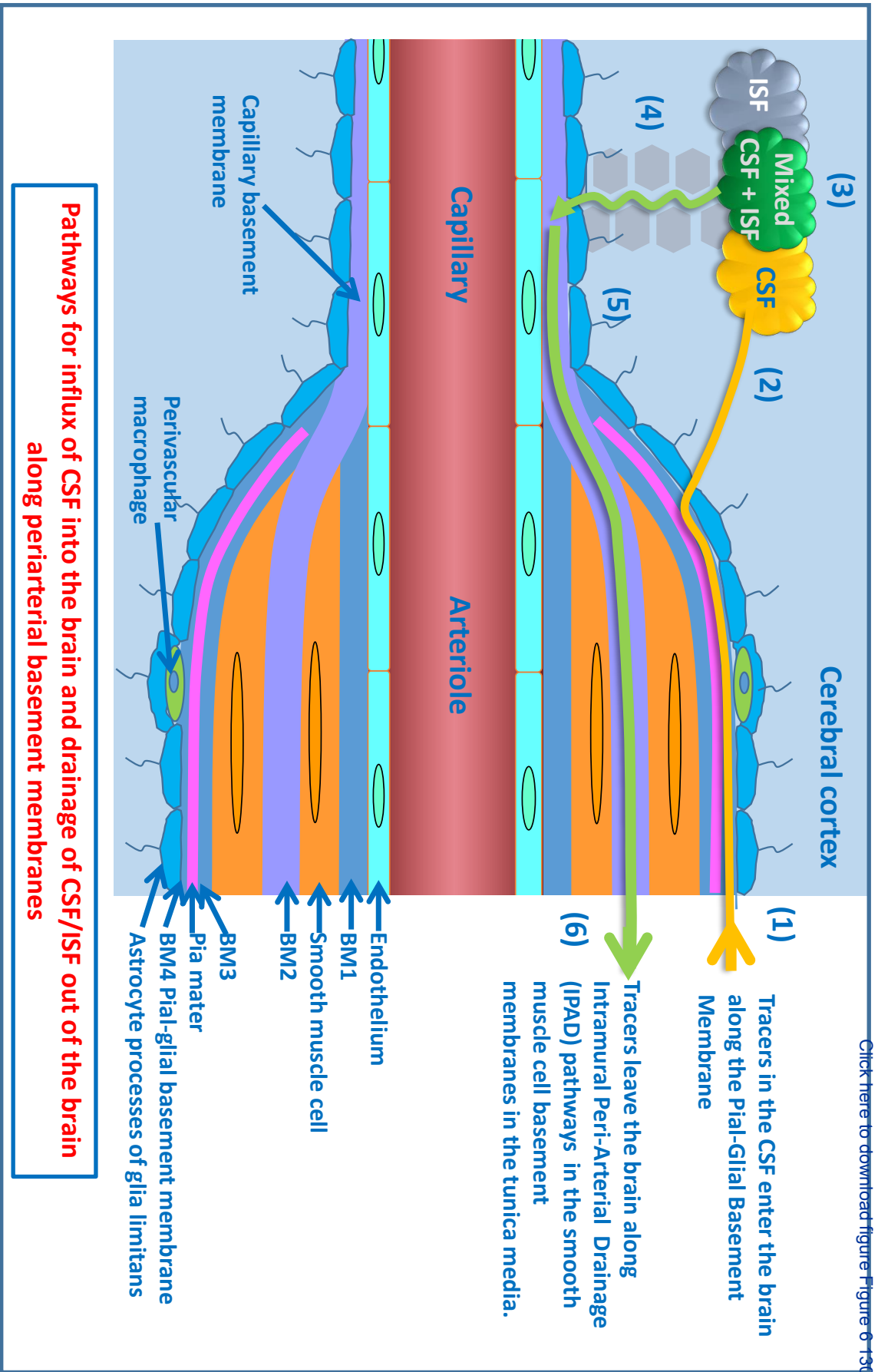






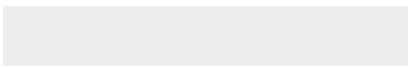








Click here to access/download  
**electronic supplementary material**  
Online Resource 1.tiff





Click here to access/download  
**electronic supplementary material**  
Online Resource 2.tiff





Click here to access/download  
**electronic supplementary material**  
Online Resource 3.tiff

